

gBuilder: A Scalable Knowledge Graph Construction System for Unstructured Corpus

Yanzeng Li, Lei Zou

Wangxuan Institute of Computer Technology, Peking University

liyanzeng@stu.pku.edu.cn,zoulei@pku.edu.cn

ABSTRACT

We design a user-friendly and scalable knowledge graph construction (KGC) system for extracting structured knowledge from the unstructured corpus. Different from existing KGC systems, gBuilder provides a flexible and user-defined pipeline to embracing the rapid development of IE models. More built-in template-based or heuristic operators and programmable operators are available for adapting to data from different domains. Furthermore, we also design a cloud-based self-adaptive task scheduling for gBuilder to ensure its scalability on large-scale knowledge graph construction. Experimental evaluation not only demonstrates the ability of gBuilder to organize multiple information extraction models for knowledge graph construction in a uniform platform, and also confirms its high scalability on large-scale KGC task.

1 INTRODUCTION

In recent years, the knowledge graph has gained significant achievements in several areas such as recommended system[28], Natural Language Processing (NLP), and become an important part of the technology that powers artificial intelligence. For example, there were a large number of researches targeting knowledge bases question and answer (KBQA)[31, 66, 83] and utilizing the knowledge graph to enhance pre-trained language models (PLM)[46, 87], or some specific NLP applications. Meanwhile, the demand for knowledge graph resources has also promoted research on knowledge graph construction (KGC) techniques and graph data management such as gStore [93], Apache Jena [74], and neo4j [60]. In general, the most common used knowledge base backbone is DBpedia[4], Freebase[9] and YAGO[30], which are built by manual and rules. However, for specific domain applications[1] such as medical, agricultural, and financial, domain-specific knowledge bases are required, which puts great demands on KGC. There was a lot of previous research related to domain knowledge graph construction such as ontology learning[3, 8], information extraction[16, 47], and knowledge base system design[36, 80, 88]. However, there is few unified systems to support domain experts to conduct the tedious KGC tasks except for only a few proposals (DeepDive[80]), but these existing KGC systems only embed fixed IE (information extraction) components and pipeline, but sacrifice the capability of embracing the rapid development of IE models. There are two motivations of our proposed KGC system gBuilder. First, we abstract NLP models and operators from the perspective of system and design a unified and flexible KGC framework that can involve any IE model. The graphic workflow design facilitates domain experts to design KGC tasks without the knowledge of complicated IE models and coding

from scratch. Second, KGC is a computation intensive task and gBuilder is a cloud-native system. Thus, considering the features of IE tasks in KGC, we propose a series of effective task schedules.

Traditionally, building a knowledge graph is based on manual annotation or expert systems[14, 38, 62], but it is often laborious and only adapt to small scale corpus. Therefore, researchers adopted some rule-based methods[4, 9, 30] to obtain structured knowledge from un/semi-structured text to build knowledge graphs. Benefiting from the development of machine- and deep learning techniques, a large amount of NLP studies on information extraction (IE) have appeared in recent years. Deep learning-based models can be trained by supervised datasets or other paradigms, to extract entities or relations from text with high accuracy. In particular, PLMs have taken the performance of IE models to a new level[20, 56, 75], which lays a solid foundation for extracting knowledge from the unstructured corpus. In the last decades, deep learning-based techniques are widely conducted in knowledge extraction, refinement, completion, alignment, etc[23].

Recently, how to design KGC's pipeline and how to organize various IE models has become a new problem, thus KGC systems emerged[12]. The most well-known KGC system is DeepDive[80], which is a data management system to populate the structured knowledge base with knowledge extracted from the unstructured corpus. For materializing KGC, DeepDive introduced techniques such as feature engineering and human-in-the-ai-loop, and employed a SQL-like high-level declarative language to describe the data pipe and models. Although the latest KGC systems such as DeepDive implemented building knowledge graph, they still have room for improvement: 1) most existing KGC systems use methods such as heuristic rules and probabilistic statistical models to extract entities and relations, and do not take advantage of SOTA's deep learning models. 2) most KGC systems do not consider the scalability and performance of the inference process, which is inefficient in large-scale KGC. 3) users are restricted to the paradigm of the KGC system, with narrow operating space and lack of flexibility. 4) most KGC systems use a high-level declarative language to describe the KGC workflow, it brings a high threshold for common users.

To tackle the aforementioned limitations, we propose gBuilder, a KGC system with usability and scalability features. Specifically, gBuilder provides user-friendly visual and interactive KGC workflow design tools, and implements any form of KGC through built-in operators and deep learning IE models, with the addition of user-trained models or custom-programmed operators. To ensure scalable of KGC, gBuilder adopt cloud distribution architecture and provides efficient and reliable distributed scheduling to boost the efficiency during the inference phase.

Compared with existing KGC systems such as DeepDive[80] and T2KG[36], our system features high scalability and high performance, extending capabilities by adopting multi-cloud computing, and providing more functions for KGC. Compared with existing distributed computing systems such as Spark[77] and Flink[13], our system designs and implements a large number of specific operators and built-in well-trained information extraction models specifically for KGC scenarios, and designs distributed scheduling for the characteristics of information extraction applications. Compared with distributed deep learning (DDL) scheduler such as Tiresias[27], BytePS[32], etc., our system focus on the more coarse granularity of scheduling, which is for an ensemble of different architectures deep learning models.

We summarize the contributions of this paper and the proposed system in the following points: (1) We investigate the practical process of KGC and propose a system, called gBuilder, for building-up KGC workflow and data pipeline flexibly, and achieve the goal of building the knowledge graph with low cost and little background knowledge for common users. (2) We investigate the deep learning-based information extraction models and the theory of ontology merging, and provide a series of built-in template-based, heuristic-based and programmable operators for adapting built-in models and data from different domains. Experimental results on benchmark datasets demonstrate the effectiveness of KGC workflow in gBuilder which ensembles multiple monolithic models and operators. (3) We adopt the multi-cloud distributed solution and design a cloud-based self-adaptive task scheduler according to the characteristics of NLP information extraction tasks, which enabling the scalability on large-scale KGC. Read-world experiments prove the effectiveness of our method on both economy and performance.

In addition, we design a user-friendly drag-and-drop interactive interfaces for designing the KGC process, as well as provided operation interfaces such as data management and model management. In the beta test, our system provided high-quality service for users, and verified the usability and stability of this system.

2 PRELIMINARY & RELATED WORK

Knowledge graph construction (KGC) studies have emerged in recent years, including the ontology design for various domain-specific knowledge graphs [1, 35], the KGC by top-down [30] or bottom-up [4] approaches, and the utilization of NLP methods such as deep learning IE (information extraction) models [68, 94] to extract structured information from unstructured corpus. In this paper, based on abundant IE models, we design gBuilder, a KGC system focusing on choreographing the models and operators to implement the whole KGC task. Before digging into details, we first introduce preliminary knowledge as well as related work.

Knowledge Graph (KG). Knowledge Graph [23] uses a graph-structured data model to store and govern linked data and can explicitly describe the semantics for the connection of structured data. Typically, Resource Description Framework (RDF)¹ is the de-facto standard of KG, representing KG as a collection of triples (*subject, predicate, object*) (abbreviated as (*s, p, o*)), which defines

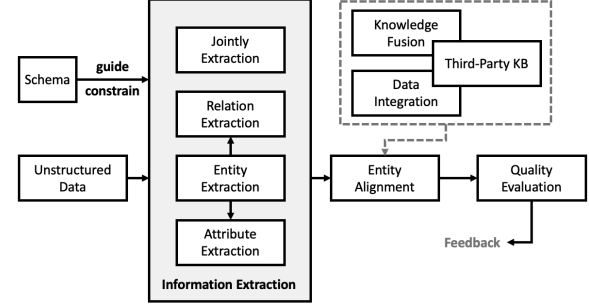


Figure 1: The illustration of top-down KGC from unstructured text. Which gBuilder mainly concerned is the grey highlighted information extraction part.

the relation between two entities (*s* and *o*) or describe the attribute of an entity (*s*).

Ontology. The Ontology defines the data patterns and characterizes the high-level conceptualization of the formal semantics of a KG, which can be regarded as the *schema* of the data. With the guidance and restriction of a well-defined ontology, the process of KGC would be normalized and the constructed product would be consistent. Specifically, the ontology specifies the target entities, relations and attributes to extract [2]. In applications, ontology can be constructed manually by experts and many ontology design tools are available, including Protégé [51]. In this paper, we focus on the information extraction phase of KGC and assume that an ontology has been explicitly defined.

Knowledge Graph Construction (KGC). Building a KG from an unstructured corpus is a critical technology path to building up a more complete and larger-scale knowledge graph [17, 89]. KGC is generally categorized into two approaches: top-down and bottom-up. The top-down approach means the target ontology is well-defined, and then knowledge instances obeying the ontology are appended into knowledge base [89], while, the bottom-up scheme extracting knowledge instance directly and the ontologies are summarized from populated instances [41]. gBuilder belongs the former one. Figure 1 demonstrates the mainstream top-down KGC process. Note that the whole KGC lifecycle should also include knowledge fusion and KB (knowledge base) quality control, but these are beyond the scope of this paper. We focus on the IE (information extraction) component in this paper, which extracts the knowledge instances under the guidance of the target ontology.

Generally, IE is an NLP task that involves extracting structured data from unstructured or semi-structured text. In order to automatically acquire knowledge instances including entities, relations, and attributes, numerous IE tasks are extensively studied.

Named Entity Recognition (NER) aims to extract mentions of rigid designators from text belonging to pre-defined semantic types such as person, location, organization [42, 52]. The entity is the essential node in the knowledge graph, and the quality of entity extraction (precision and recall) greatly impacts the quality of follow-up tasks for knowledge acquisition.

Relation Extraction (RE) refers to extract the relationship for entity pairs. In the pre-defined schema scenario, it is usually treated

¹<http://www.w3.org/RDF/>

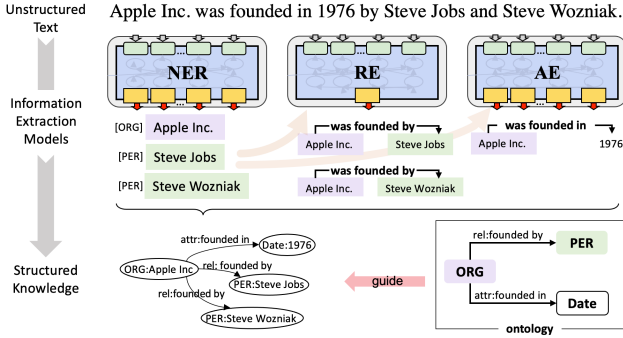


Figure 2: The example of gBuilder KGC with multiple deep learning IE models and guided by pre-defined ontology.

as a classification task to predict the relation category according to evidence text containing mentions of the entity pair [39]. The triples constituted by relations are the fundamental instance in the knowledge graph, and the performance of RE is directly related to the accuracy of edges and connectivity of the knowledge graph.

Jointly Extraction (JE) is an emerging IE approach in recent years, and it aims to detect entity pairs jointly along with their relations by a single model. JE is treated as a supervised learning task based on structured annotation, and it usually gains better performance on specific datasets due to more supervisory signals, and JE eliminates cascading errors in the NER-RE pipeline utilizing the superiority of the joint monomer model [5, 72]. In IE for KGC, there is a trade-off between JE’s high performance and its relatively rigid output structure.

Attribute Extraction (AE) is a task to identify the literal attribute and the corresponding attribute value for a specific entity from unstructured text. AE can be divided into attribute value extraction and attribute extraction [82]. The former can be solved by the regex matching or the neural network similar to NER, and the latter can be solved simultaneously with RE and JE [72], or designed heuristic rule [50, 67].

As illustrated in Figure 2, the above IE models work cooperatively to accomplish their respective duties, and structured knowledge can be extracted from unstructured text.

Challenges of IE tasks in KGC: The NLP community has proposed a wide variety of IE models in recent years, which are claimed to achieve SOTA² on various datasets. However, the existence of those different IE tasks, model structures, datasets, and different training hyperparameters brings enormous diversity, which causes difficulties in organizing KGC by simultaneously exploiting the respective strengths of models.

The diversity of IE tasks and dazzling array of NLP models bring uncertainty and pose challenges to KGC, especially when domain engineers lack of ML (machine learning) and NLP experience. That is the bottleneck of KGC in real applications. Existing KGC systems [80, 84] perform KGC processes such as relation/attribute extraction under a fixed paradigm and did not take advantage of the latest SOTA IE models. For example, DeepDive [80] proposes heuristic extraction rules and statistical learning-based rule scoring strategies,

but fail to employ SOTA NLP models. Even the latest work DeepKE [84], which introduces deep learning models for KGC in various scenarios (e.g., low-resource), is still under a fixed KGC paradigm and cannot utilize the inexhaustible SOTA IE models for building the universal KGC workflow.

To enable KGC process in a manufacturer model, we should develop a **Unified Information extraction (Uniform for short)** paradigm in gBuilder system to address the following technique challenges of IE tasks in KGC: (1) how to build a detachable and replaceable system to embrace the rapid development of IE models in the NLP community rather than with fixed models; (2) how to abstract the diverse IE tasks and models in a normalized form and how to design a low-code interface for KGC in a friendly and flexible way; (3) last but not least, the efficient processing of IE tasks is also vital in KGC pipeline.

3 SYSTEM OVERVIEW

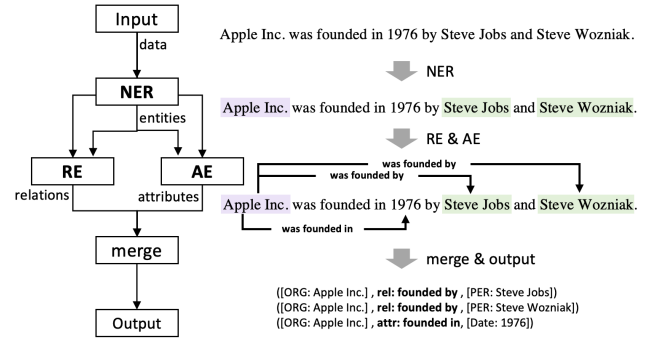


Figure 3: The example of flowline (left) and the corresponding extraction process (right) of Uniform.

In this paper, we focus on the unified information extraction paradigm (Uniform) that is the core component of gBuilder³. Specifically, first, a user needs to input the target ontology of KG as well as the corpus. A running example of the ontology and the original sentence is given in Figure 2. Second, based on the user-specific requirements of KGC and the characteristics of the target knowledge base, the user is asked to design a DAG (directed acyclic graph)-like flowline (Definition 4.1), which is an abstraction of workflow and data pipeline in KGC. A flowline includes nodes corresponding to IE models and operators that are needed for KGC (Section 4). Those nodes are connected according to the user-controlled data flow in KGC. For example, Figure 3 shows a brief flowline that defines the extraction process in Figure 2, by posing models like NER, RE and AE cascadingly and connecting them by the data pipeline. Third, the designed flowline, ontology, and target corpus are submitted to the gBuilder, and the system will perform validation for them, and schedule the flowline automatically. The flowline of the KGC execution plan would be split into several parallelable subgraphs and executed on distributed cloud computing nodes. The details of optimizing task scheduling and distributed execution for KGC flowline to balance the performance and cost are studied in Section

²SOTA: state-of-the-art

³The detail of system architecture is attached in Appendix.

5. Finally, by the time the whole corpus is processed through the flowline, the extracted triples can be stored in a graph database for further graph analysis.

4 FLOWLINE

4.1 Normalized IE Models

As Section 2 described, there have been various studies on IE in recent years, including NER, RE, etc. Furthermore, the settings of different IE tasks are widely divergent. How to organize those algorithms and models with different settings, model structures, and output formats is a challenge. To normalize these IE models, we categorize them into two types according to the orientation of the IE models:

(1) *Classification-based model CC*, which outputs a category label:

$$CC(x_i) = \hat{y}_i, \quad (1)$$

where C represents classifier, x_i denotes the i -th sample and \hat{y}_i denotes the i -th category label. The tasks or subtasks related to predicting the predicate are divided in this CC category, including RE, attribute name extraction in AE, relation extraction in JE, etc. Even if the model originally outputs the spans, we will unify it into the CC paradigm by building a label set dictionary.

(2) *Chunk Extraction-based model CE*, which outputs a set of fact phrase chunks:

$$CE(x_i) = \hat{Y}_i = \{\hat{y}_{i1}, \dots, \hat{y}_{i|\hat{Y}_i|}\}, \quad (2)$$

where CE represents chunk extractor, and \hat{y}_i is the extracted fact from the sample x_i . The tasks or subtasks related to subject or object extraction are classified in this CE category, including NER, attribute value extraction in AE and entity extraction in JE, etc. The above abstraction smooths out the logical differences caused by diverse models, such as sequence tagging, slot filling, and heuristic pattern matching.

Built-in Models. Follow the principle of above mentioned normalized form, we prepared some built-in IE models for startup. A single deep learning-based IE model that can be used for inference can be viewed as two parts: model structure, and well-trained model parameters (or weight). In gBuilder, we use (m, d_t, hp) to identify a model, where m is the whole model, including model structure and initialized parameters, d_t denotes the training dataset, and hp is the hyperparameter used to configure the training details. Implicitly, d_t also defines the label set of a model. d_t and hp directly impact the tuned parameters of the model after training, and the performance of well-tuned model in the inference process. For the sake of ease of use, we train different models on different datasets in multi-linguals and multi-tasks. These models include classical and state-of-the-art models and popular repositories from academic or industrial open-source projects. In order to make the maximum utilization of the precious supervised training datasets, and to provide users with as many diversified well-trained models as possible to reinforce model ensemble[91], the “matrix” of built-in models approximately presents a combination of $M \times D_t$ ($M = \bigcup m, D_t = \bigcup d_t$), while the respective hyperparameters hp are provided by the original author of model or fine-tuned by ourselves through automatic or manual tuning. With this strategy, we provide a large number of built-in models in the model hub of gBuilder and a part of employed datasets

for well-tuning built-in models, which are shown in Table 6 and 7 of Appendix. The “matrix” of built-in models is also illustrated as Figure 13 of Appendix.

Custom Model Training is a requisite for adaption of domain-specific KGC, especially when the built-in models cannot meet the requirements of the ontology of the target domain. gBuilder provides abundant methods for custom model training. Users can invoke the custom model training function within gBuilder, or self-service registering a user-made model that is technology- and structure-agnostic to gBuilder, and providing inference service by the promissory interface for responding to the remote call from gBuilder system.

gBuilder provides two training modes for users: 1) using a built-in well-trained model and uploading more data for continuous learning; 2) using a built-in model structure, uploading training dataset and label sets, then training it from scratch. For this mode, gBuilder provides three strategies for tuning the hyper-parameters: using the default parameters of the built-in model; using user custom hyper-parameters; using the built-in automatic hyper-parameter selection method (including grid search, simulated annealing, etc.).

Generally, the precision of KGC would be substantially improved after training a custom model using the corresponding supervised training dataset that conforms to the target KG domain.

Custom Model Endpoint Register. gBuilder opened up an interface to advanced users, allowing users to register their self-serve models or algorithms and plug into the gBuilder KGC flowline in an agreed-upon format of data and endpoint state. It provides more flexibility to allow users to build and train models by themselves with better performance or to implement more complex machine learning data pipelines such as active learning⁴.

4.2 Unite Models and Ontology Merging

In the practice of KGC, although training a custom model can provides better precision, it is often high-costly and even infeasible for domain engineers due to lack of ML (machine learning) and NLP experience. A desirable approach is to unite build-in models to conform to the target KG ontology and use them directly without training custom models. However, well-tuned build-in models are often inconsistent with the target ontology, and the distribution of training data usually deviates from the target domain. To mitigate this phenomenon, we introduce and integrate multiple build-in IE models in gBuilder, and it is primarily geared towards choreography and fusion of these build-in models that are trained on different corpora with label sets.

The output of deep learning IE models are usually discrete categories and can be treated as a flat structured ontology. The problem of uniting different IE models can be regarded as merging multiple ontologies into a target ontology. Traditionally, ontology merging needs to find the semantic relationship between concepts of different ontologies [29, 33, 63]. Within the scope of the flat ontology of IE models, regardless of the hierarchical and heterogeneous structure, ontology merging is relatively straightforward. We define four atomic operations to cover most of the ontology merging situations in Figure 4. **filter**: pruning a set of classes or relations (defined as F

⁴We released a repository (<https://github.com/pkumod/gbuilder-endpoint-example>) of a minimal implementation of custom model endpoint for guiding development.

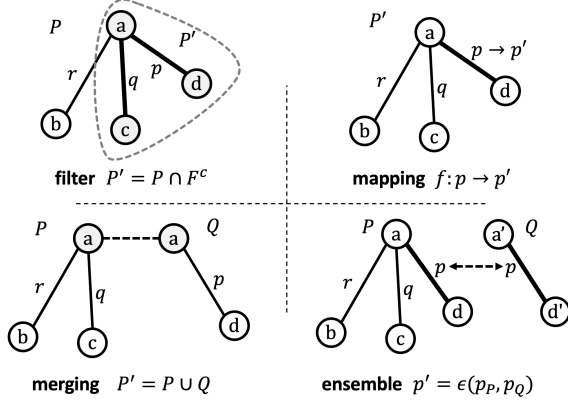


Figure 4: The illustration of four primitive operations of ontology merging in gBuilder.

in the graph) that are not related to the target ontology. **mapping**: literally mapping the concept name of the original ontology to the target ontology. **merging**: directly merging multiple ontologies with non-overlapping concepts. **ensemble**: adopt model ensemble approaches to address the overlapping concepts (including classes or relations) in multiple ontologies.

Through the flexible combination of these noncommutative operations to form a merging plan, gBuilder is sufficient for most situations of ontology merging. The merging plan is described by flowline (that will be discussed in Section 4.3) and constructed by some of built-in operators. After constructing the merging plan at the ontology level, gBuilder will follow this plan to transform and merge knowledge instances output from well-tuned IE models in the KGC process.

Model Ensemble Tailored for IE Models. In order to deal with the redundancy of multiple models outputting the analogical class during ontology merging and improve the prediction performance by integrating multiple well-tuned models with different architectures and trained on the different corpus, gBuilder introduces model ensemble for inference process.

(1) *Model ensemble applied in classification-based tasks.* Model ensemble is intrinsic suitable for classification-based models like relation classification. Therefore, the basic method of model ensemble can be used to solve the integration of those classification-based IE models. There are also two built-in ensemble operators in the gBuilder, one is based on vanilla majority vote:

$$\hat{y}_i = \text{mode}\{C_j(x_i) | j \in \mathbb{N}_+, j < m\}, \quad (3)$$

where m denotes the number of classifiers, $C_j(\cdot)$ denotes the j -th classifier' prediction label, mode is for counting the most frequent labels. The other is the score-based ensemble, which aims to gain the final predicted label by the weighted score sum among all classifiers for each label. The highest score label would be treated as the final results, and a threshold is introduced for filtering the unreliable predication. The score-based ensemble is shown as:

$$\hat{y}_i = \begin{cases} \arg \max_k \sum_{j=1}^m w_j p_{i,k}^j, & \text{if } \forall p_{i,k}^j > \delta \\ \text{reject} & \text{otherwise,} \end{cases} \quad (4)$$

where w_j denotes the weight of the j -th classifier (this weight is specified by the user, by default it is $1/m$). $p_{i,k}^j$ denotes the score that the j -th classifier predicting the i -th sample into the k -th class, δ is the threshold to accept the predicted label (by default it is 0.5), if all prediction score below this threshold, the corresponding sample will be ignored, e.g. in relation classification task it will be marked as *no relation* between entities.

(2) *Model ensemble applied in extraction-based tasks.* The sequence tagging model is more diverse and complicated, and it is difficult to apply a unified score to measure the confidence coefficient of sequence tagging's prediction. Recently, some researches [42] proposed sequence tagging-based model ensemble approaches based on encoder [53] or tag decoder [15]. However, these inner-model ensemble methods require specific model structures and not easy to transfer across different domains, and it is over fine grain and incompatible with gBuilder, which is based on the well-tuned model pipeline. Therefore, based on our introduced *CE* extraction paradigm, we implement ensemble outside of models by merging and deduplicating extracted chunks directly. In this way, we can introduce multiple models in extraction-based tasks like NER, which improve the recall score as possible to minimize cascading errors for the overall knowledge extraction pipeline.

Inevitably, this manner would produce some exceptional cases such as redundant nested named entities. Those special cases are delivered to the post-processing, including knowledge graph quality control, entity disambiguation. Experimental results have shown that this manner does not harm the overall accuracy of knowledge instance extraction.

Built-in Operators. For the implementation of uniting different models, besides *filter*, *mapping*, *merging* and *ensemble*, we propose a series of *built-in operators* are preset in gBuilder, allowing users to build the flowline (Section 4.3) conveniently. Table 8 in Appendix G demonstrates the functions, inputs, and outputs of the most of built-in operators in details. These built-in operators can be flexibly combined to implement the features required by KGC.

4.3 Flowline: Choreography of Operators

With the built-in models for extracting information and the built-in operators for uniting these models, the KGC pipeline can be described in an abstract form, called *Flowline* in gBuilder, a combination of IE workflow and data pipeline.

Definition 4.1 (Flowline). *Flowline* is a Directed Acyclic Graph (DAG) that abstracts KGC workflow in which (1) each vertex represents a IE model or an build-in operator. Note that each node is also called a *task*; (2) an edge defines the data flow between the two corresponding tasks; (3) there are a single *entry vertex* and a single *exit vertex* that correspond to the start and the end of a flowline, respectively.

Once the flowline is determined, the resource estimation of each node in the workflow will also be determined, and the system can schedule such a DAG to ensure the entire flowline is completed as soon. We will propose a DAG-partition strategy to optimize

optimizing flowline schedule in the cloud-computing environment in Section 5.

Use Case of Designing a Flowline. To explain clearly the design of flowline, we conducted a case study with the example of extracting knowledge instances in Figure 2, and Figure 5 shows the flowline we have designed for this purpose.

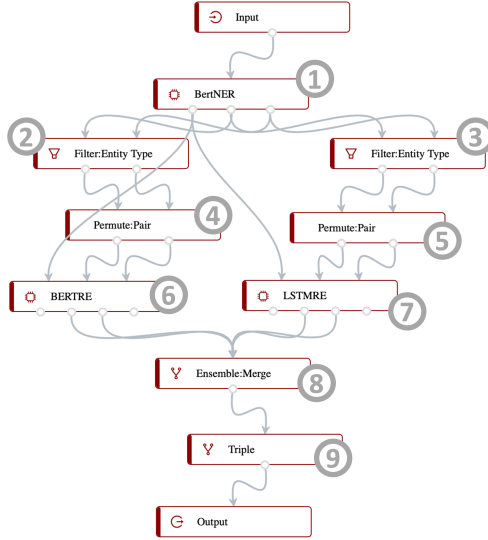


Figure 5: Flowline example. For convenience we have added numeric symbols to each task node.

From a holistic perspective, to extract knowledge instances, we must first obtain the entities in the text. So we arrange the built-in BertNER model (1), which is a high-performance NER model selected, with the ability to extract the person’s name, location, organization name, and some of the attributes (Date, Time, etc.), which meets the requirements of the pre-defined ontology.

After further research, it was found that the model hub contains an RE model named BERTRE (6) that specializes in identifying relations between company and person, as well as an RE model named LSTMRE (7) that can identify attributes relation of company founded date. Therefore, we chose to make branches off in flowline for identifying person-organization relations and organization-(founded date) attribute relations to exploit the specialty of these two models, respectively.

For this purpose, we employ filter nodes (2,3) to split the data by entity type and then transform the entities into entity pairs through “permute:pair” nodes before feeding entity pairs into the RE models (6,7). After identifying relations and attributes, we use an Ensemble node (8) to integrate the results and then go through the triple constructor (9) to get the final structured knowledge instance in the form of the RDF triple.

To facilitate defining the more complex Flowline and the migration, we have defined a domain-specific language called Graphical Flowline Language (GFL) to describe a flowline formally, which is interchangeable with the visual flowline. GFL is detailed in Appendix C and the designed visual flowline in Figure 5 is congruent with GFL in Listing 1 of Appendix C.

5 TASK DISPATCHING

Handling a KGC project with multiple deep learning models requires large-scale heterogeneous computing resources (including CPUs and GPUs, etc.), and furthermore, providing such massive KGC services to numerous users poses a huge challenge to the computing resources. Therefore, gBuilder adopts cloud computing architecture and employs the auto-scaling feature to provide users with high-quality services. As a cloud distributed system, the scheduling of tasks will directly determine the scalability, Quality of Service (QoS), resource utilization, and the monetary cost of cloud procurement. This section focuses on task dispatching in gBuilder.

5.1 Micro-batch Distributed Cloud Computing

To minimize the impact of the data transmission delay between cloud VMs on the time overhead of the overall flowline, a micro-batch-based data layout is designed to reduce the proportion of transmission time within the overall flowline and a task-oriented column-based transmission is employed to reduce the data size at intermediate computing nodes.

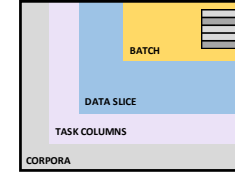


Figure 6: The data hierarchical layout of gBuilder.

5.1.1 Data Layout. The data layout in gBuilder is defined as four levels, as shown in the Figure 6.

- *Corpora* contains all documents of an entire project.
- *Task Column* is a set of data columns related to a single task, which only contains the required fields. We split the data into columns and then group/transmit the necessities for successor tasks to reduce the intermediate transmission data amount (e.g., a single *entity_type_filter* task only requires the input of *entity_type* and only the corresponding data column from precursor tasks would be transferred to this computing node).
- *Data slice* is an essential data transmission unit (i.e., *micro-batch*⁵) between a task (i.e., a vertex) and its successor in the flowline. The size of the data slice is determined by the system environment. Within the data slice, data rows can be order-preserved. Data slices could be distributed to different tasks and asynchronously invoked to save data transfer time [71, 78].
- *Batch* is identical to the concept of batch learning. By batching the data, the dedicated computing hardware (like GPU, TPU) can maximize the acceleration of matrix calculations to increase the speed of deep learning model inference or training [18].

5.2 Problem Formulation

5.2.1 Flowline Model. To model the whole processing time of a flowline (i.e., a DAG, see Definition 4.1), we introduce vertex weight

⁵It is named as “data slice” to avoid counter-intuitiveness with the concept of “batch” in batch learning.

Table 1: Common used notations in Flowline scheduling.

Notations	Definitions
$G = (V, E)$	A DAG with a vertex set $V = (v_1, v_2, \dots, v_i)$ and an edge set $E = (e_1, e_2, \dots, e_j)$
t_i	Task t_i in Flowline, which is interchangeable with vertex v_i in DAG G
$ D $	The size of corpora D
$ slice $	The size of micro-batch data unit (data slice)
T	Task list of Flowline, $T = \bigcup t_i, T \equiv V$
V^m, V^o	Sub-list of GPU- and CPU-intensive tasks/vertices
vm	Cloud Virtual Machine
$N(v)$	Neighbour node set of vertex v
$N_{in}(v), N_{out}(v)$	Precursor and successor node set of vertex v
$w(v_i)$	Weight of vertex (equal to the execution time of task v_i)
$w(\overrightarrow{v_i v_j})$	The time of unit data transferring from task t_i to t_j
$FT(t_i)$	The finish time of task t_i
$M(G)$	<i>makespan</i> , the running time of processing a unit data for entire DAG G

$w(v_i)$ and edge weight $w(\overrightarrow{v_i v_j})$ to represents the excepted computation time of task t_i (corresponding to vertex v_i) and the micro-batch data transmission time from task t_i to t_j . Note that we ignore edge weight between v_i and v_j (i.e., $w(\overrightarrow{v_i v_j}) = 0$) if the two tasks are executed at the same VM. We only consider the data transmission time among different VMs.

gBuilder online applies for requested cloud resources to execute a flowline job. Given a flowline DAG $G(V, E)$, we assume that there are $|V^m|$ IE model vertices and $|V^o|$ operator vertices in G and each IE model vertex needs a GPU card and each operator vertex needs a CPU core. To better motivate our task scheduling, we first consider the following ideal case.

Ideal Case. Given a flowline DAG G over corpora D , in the ideal case, we assume that we can apply for a powerful virtual machine (VM) with enough GPU cards ($\geq |V^m|$) and CPU cores ($\geq |V^o|$) and we do not care the monetary cost. As mentioned earlier, we adopt the *micro-batch* scheme (Section 5.1) and one data slice is an data transmission unit. Therefore, the total processing time can be evaluated as follows:

$$Time(G, D) = \frac{|D|}{|slice|} \cdot M(G) \quad (5)$$

where $|D|$ and $|slice|$ denote the data volume of the whole corpora D and one data slice size, and $M(G)$ denotes *makespan*, which refers the running time of processing a data slice through the entire DAG G . $M(G)$ is equal to the *finish time* (FT) of the exit vertex t_{exit} , where the *finish time* for any vertex v_i in DAG D as follows:

$$FT(v_i) = \begin{cases} w(v_i), & \text{if } v_i \text{ is the entry vertex in DAG } G. \\ w(v_i) + \max_{v_j \in N_{in}(v_i)} (FT(v_j) + w(\overrightarrow{v_i v_j})) & \text{otherwise.} \end{cases} \quad (6)$$

where $N_{in}(v) = \{u \in V, e_{(u,v)} \in E\}$ denotes the precursor vertices of v . Essentially, *makespan* is weight sum of all vertices and edges

along the *critical path*⁶ in G . Note that all tasks are resident at one VM in the ideal case, thus, all edge weights are zero in G .

Partition-based DAG Scheduling. Obviously, the above assumption is not practical. First, there may not be a powerful VM equipped with enough resources, such as GPU cards. Second, the price of one powerful VM with the full-size capability is much higher than the total monetary cost of multiple VMs with low resources. We will discuss the pricing model in cloud service vendors later (Section 5.2.2). Therefore, a desirable solution is to employ the DAG partition strategy to balance the performance and the total monetary cost.

Definition 5.1 (Partition). A *partitioning* of a given DAG flowline $G = (V, E)$ is an edge cut-based partition $\pi = \{\mathcal{G}'_1, \mathcal{G}'_2, \dots, \mathcal{G}'_k\}$, where each $\mathcal{G}'_i(\mathcal{V}_i, \mathcal{E}_i)$ is a small DAG and $\mathcal{V}_i \neq \emptyset$, $\bigcup_{i=1}^k \mathcal{V}_i = V$ and $\mathcal{G}_i \cap \mathcal{G}_j = \emptyset, 1 \leq i \neq j \leq k$.

Given a partition $\pi = \{\mathcal{G}'_1, \mathcal{G}'_2, \dots, \mathcal{G}'_k\}$ over a DAG flowline G , we apply for k VMs and each one accommodates one sub-DAG \mathcal{G}'_i . Due to the data transmission between different VMs, we should consider edge weights if the corresponding tasks are resident at different VMs. Formally, we have the following definition.

Definition 5.2 (Partition-based Computation Graph). Given a partition $\pi = \{\mathcal{G}'_1, \mathcal{G}'_2, \dots, \mathcal{G}'_k\}$ over a DAG flowline $G(V, E)$, the corresponding *computation graph* $G'(\mathcal{V}', \mathcal{E}')$ is defined as follows:

- G' has the same vertex and edge sets with G ;
- Each vertex v' in G' has the same vertex weight with the counterpart in G ;
- Each edge weight $w(\overrightarrow{v'_i v'_j})$ is defined as follows:

$$w(\overrightarrow{v'_i v'_j}) = \begin{cases} \sim 0, & \text{if tasks } t_i \text{ and } t_j \text{ are in the same VM.} \\ L_{v'_i, v'_j} + \frac{\text{Data}_{ij}}{\beta_{i,j}} & \text{if tasks } t_i \text{ and } t_j \text{ are in different VMs.} \end{cases} \quad (7)$$

where Data_{ij} denotes the size of data slice transferred from v_i to v_j , $\beta_{i,j}$ represents the bandwidth between two VMs and $L_{v'_i, v'_j}$ is the network latency;

Based on the partition-based computation graph G' , we can know the whole processing time:

$$Time(G', D) = \frac{|D|}{|slice|} \cdot M(G') \quad (8)$$

where $M(G')$ denotes the *makespan* of partition-based computation graph G' . Note that different partitioning over G may lead to different $M(G')$. Therefore, we formally define our DAG-based partition problem.

Definition 5.3 (DAG Partition). The DAG partitioning problem is to find the *optimal partition solution* $\pi = \{\mathcal{G}'_1, \mathcal{G}'_2, \dots, \mathcal{G}'_k\}$ for DAG G , which should satisfies the qualification ω and minimize the objective function J , where

- (1) The qualification condition ω refers to the resource constraint, i.e., each VM M_i has no less than $|V_i^m|$ available GPU cards and $|V_i^o|$ CPU cores, $i = 1, \dots, k$, where $|V_i^m|$ and $|V_i^o|$ denote the number of IE models and operators in sub-DAG \mathcal{G}'_1 that is resident at VM M_i ;

⁶The longest weighted path in the DAG is critical path, which determines the total runtime of the workflow.

(2) The optimization objective is defined as

$$\arg \min_{\pi} J(G, \pi). \quad (9)$$

In the context of cloud computing, the optimization function $J(G, \pi)$ should consider the total processing time (Definition 8) as well as the monetary cost. We will discuss the pricing model as follows.

5.2.2 Cloud Computing Pricing Model. The pricing model determines the monetary cost of gBuilder as a cloud-based system, which would put a significant impact on task scheduling designing [54]. *G4 instance*⁷ in Amazon Elastic Compute Cloud (AWS EC2) is the industry's most cost-effective GPU instance for machine learning inference and graphics-intensive applications among EC2 product family [37], therefore we take g4dn (Nvidia GPU series) as an example to investigate the quotation of GPU cloud instances in the pay-as-you-go (on demand) pricing manner.

We take the number of CPU cores and GPU cards as parameters and hypothesize that they are combined in a linear relation [11]. The price can be expressed as Equation 10.

$$Price_{vm}(\#CPU, \#GPU) = \theta_1 \times \#CPU + \theta_2 \times \#GPU \quad (10)$$

where $\#CPU$ and $\#GPU$ denotes the number of CPU cores and GPU cards, θ_1 and θ_2 are two fitting coefficients.

Table 2: Multiple linear regression equation of the CPU-GPU number applied to estimate the price of Amazon EC2 g4dn instance family, with $\theta_1 = 0.0565$ and $\theta_2 = 0.3$.

Instance	GPU num	CPU cores	Unit Price (per hour)	Estimated (per hour)	Error (%)
g4dn.xlarge	1	4	\$0.526	\$0.526	0%
g4dn.2xlarge	1	8	\$0.752	\$0.752	0%
g4dn.4xlarge	1	16	\$1.204	\$1.204	0%
g4dn.8xlarge	1	32	\$2.176	\$2.108	3.13%
g4dn.16xlarge	1	64	\$4.352	\$3.916	10.02%
g4dn.12xlarge	4	48	\$3.912	\$3.912	0%
g4dn.metal	8	96	\$7.824	\$7.824	0%

Easily-accessible statistical and experimental results of instance unit price estimation are shown in Table 2. As can be seen, Equation 10 has a minimal error rate (<5%) for most of the instances under the setting of $\theta_1 = 0.0565$ and $\theta_2 = 0.3$, where θ_1 and θ_2 can be regarded as the unit price of CPU and GPU in the AWS quotation, respectively, which also proves that CPU and GPU are the main factors affecting pricing in the cloud computing scenario⁸. In a nutshell, the parameter estimated multiple linear regression and Equation 10 can be used as the foundational element for controlling monetary costs when designing optimization objective.

⁷<https://aws.amazon.com/ec2/instance-types/g4/>

⁸We also investigated more pricing schemes from cloud vendors such as azure, tencent, aliyun, etc., which are all in accord with the same strategy.

5.2.3 Scheduling Objective. Let us recall our DAG partition problem (Definition 5.3) and we focus on the objective function J as follows. Given a partition $\pi = \{\mathcal{G}'_1, \mathcal{G}'_2, \dots, \mathcal{G}'_k\}$ over Flowline G , the corresponding partition-based computation graph is G' . Obviously, the objective function J should consider both the computational cost $cost_{com}$ (i.e., the total processing time) and the monetary cost $cost_{mon}$ (i.e., cloud resource procurement).

The $cost_{com}$ is defined as the total processing time.

$$cost_{com} = Time(G', D) = \frac{|D|}{|slice|} \cdot M(G') \quad (11)$$

The total monetary cost for processing an entire corpora can be denotes as:

$$\begin{aligned} cost_{mon} &= \sum_{i=1}^{i=k} Price(vm_i) \times Time(G', D) \\ &= \frac{|D|}{|slice|} \cdot \sum_{i=1}^{i=k} Price(vm_i) \cdot M(G') \end{aligned} \quad (12)$$

where $Price(vm_i)$ is the purchasing cost of VM vm_i and $Time(G', D)$ is the billing duration, which equals to the total processing time of corpora⁹.

Obviously, $\frac{|D|}{|slice|}$ is fixed when finding the optimal partition. Thus, we can only consider the unit price for processing a data slice when defining the objective function. Furthermore, simultaneous optimizing both $cost_{com}$ and $cost_{mon}$ is a typical multiobjective optimization (MO) problem, and it is hard to find a Pareto-optimal solution. Motivated by multi-criteria workflow scheduling problem [40, 64], we use weighted aggregation to formulate the MO into a single objective problem by combining the computational cost and monetary cost:

$$\begin{aligned} &\text{minimize} \quad J(G, \pi) = \eta cost_{com} + (1 - \eta) cost_{mon} \\ &\text{subject to} \quad \pi \in \omega, 0 \leq \eta < 1, \end{aligned} \quad (13)$$

where η is the preference factor that indicates the relative importance of the decision-making and it depends on the decision maker's trade-off between QoS and the monetary cost. Unfortunately, this optimization problem is NP-hard as given in the following theorem.

THEOREM 5.4. *Given a DAG G for a valid Flowline, finding the optimal graph partition to minimize Equation 13 has no polynomial-time approximation algorithm with a finite approximation factor unless $P = NP$.¹⁰*

5.3 Proposed Solution

Due to the hardness of finding the optimal DAG partition, considering IE computation features in KGC problem, we propose a heuristic algorithm for scheduling Flowline in a distributed cloud computing environment.

⁹The delay of cloud instance acquisition and termination is ignored because this delay is negligible compared with the total KGC process.

¹⁰The proof is given in the Appendix due to space limitations.

5.3.1 Algorithm Idea. Note that we do not intend to conquer the DAG partition problem in a general case in this paper. We first study IE computation features in KGC problem and we propose our solution based on these priori knowledge. Considering the pricing model, we can use Equation 10 to estimate the monetary cost of cloud procurement and resource utilization for gBuilder’s distributed computing workers. In most cases, the range of CPU-GPU ratio required by the gBuilder worker is typically from 2 to 6 (e.g., an IE model with 1 filter, 1 mapper, 1 ensemble operator, 1 data integration operator, 1 constructor operator). It supports us to choose an instance type with a CPU-GPU ratio as close to the requirements of gBuilder as possible. Cloud vendors tend to bundle rich additional resources in order to drive users to choose a high-end instance with multiple GPU cards, which will result in low resource utilization in our application scenarios. For example, if we purchase VMs in Table 2 for gBuilder, the g4dn.metal instance would cause 34.66% to 57.77% of monetary waste. Therefore, with the vast resource utilization deviation, we prefer to purchase the basic instance type with a single GPU and an appropriate number of CPU cores like g4dn.xlarge and g4dn.2xlarge to avoid superfluous CPU resources cost.

Other prerequisites that should be considered when developing the scheduler include:

- (1) Workloads that serve deep learning-based IE models consume most of the time slot in the pipeline.
- (2) The latency of network communication between cloud instances is non-negligible and heavily affects micro-batch processing execution efficiency. Conversely, the inner-instance communication can be negligible.
- (3) Empirically, An GPU-heavily deep learning IE model usually succeeds a series of lightweight operators (such as filters, mappers, etc.) for postprocessing. These operators are mainly consuming CPU resources.
- (4) A GPU cloud server always provides superfluous computing capacity such as redundant CPU cores, etc.
- (5) A deep learning-based IE model could be regarded as exclusively occupying all of the single GPU resources but only occupying 1 CPU core of the capacity for data loader.
- (6) Resource demand of “lightweight” operators can be regarded as 1 CPU core.

5.3.2 Heuristic Algorithm. Building on the above ideas, we can propose a heuristic algorithm to optimize the objective in Equation 13 and solve the hardness problem of flowline scheduling. To this end, we design a two-step algorithm: first, ensure the compounded tasks should not be separated as the unpartitionable clusters; then, determine the partition strategy and the number of clusters based on a greedy approach.

For convenience, we denote GPU-intensive tasks like IE models as V^m and the CPU-only tasks like lightweight operators as V^o . The unpartitionable “compound” is denoted as P_i .

Step 1. The Compounding Phase. Motivated by intuitive assumption 1, we construct a compounding algorithm based on bundling the GPU-intensive task and its subsequence CPU-only tasks. These subpopulations are self-contained and *should* be clustered; delimiting boundaries within those *compounded tasks* would only bring

extra communication cost without any profit. We summarize the GPU-task (IE model) guided compounding in Algorithm 1.

Algorithm 1: GPU-Intensive Task-Guided Compounding

```

Input :A Flowline  $G = (V, E)$ 
Output:A Set of Compounded Subpopulations
 $P = \{P_1, P_2, \dots, P_{|V^m|}\}$ 

1  $P \leftarrow \emptyset$ 
2 for  $t_i \in \{t | t \in V^m\}$  do
3    $P_i = \{t_i\}$ 
4   repeat do
5     for  $t' \in N_{out}(P)$  do
6       if  $t' \in V^o$  and  $N_{in}(t') \subseteq P_i$  then
7          $P_i.join(t')$ 
8   until visited all successors of nodes  $t'$  in  $P_i$  in  $G$ ;

```

Step 2. Cloud Resources Pre-allocation. For determine the procurement plan of cloud resources and allocate the tasks to the cloud instances, we dig into pricing strategy of cloud vendor and set up a simple polynomial function between the minimum makespan of KGC process and the procurement pricing of cloud resources:

$$y = g(x) = a + b(x - c)^{-1}, (a, b, c, x > 0) \quad (14)$$

where a, b , and c are the coefficients to fit which are dependent on the pricing strategy of cloud vendors, x denotes the planned unit price of a task, y denotes the estimated minimum makespan of the task according to the planned expenditure ¹¹. Substituting the hypothesis polynomial function relationship between planed unit price and minimum makespan into the objective function, it can be rewritten as:

$$J = \eta g(x) + (1 - \eta)x \cdot g(x) \quad (15)$$

it is a convex function with a global minimum at $x_0 = \sqrt{\frac{b}{a} \frac{\eta}{1-\eta}} + c$, which means the approximate optimal solution of J can be obtained if a combination of cloud instances whose summation of unit price is close to x_0 is purchased. This is a classic unbounded knapsack problem that can be solved in various manners (e.g., dynamic programming). Furthermore, it is easy to find a brute-force solution because of the small scale of combinations in this scenario). Note that if there are multiple procurement plans for the same price, it is preferable to choose a combination of high-end instances than multiple divided low-end instances if possible, due to Equation 18. The coefficients can be fitted by a few observations (e.g. Table 5 and Figure 12b) by *warm up*¹², and the simple regression analysis methods like non-linear least squares can be employed. For example, assuming the user expect a balance $\eta = 0.5$, and deploy a Flowline (as Figure 5) in qCloud (with setting of $a = 4.17$, $b = 5.15$ and $c = 23.96$), the expected price of optimal scheduling should close to $\sqrt{\frac{b}{a} \frac{\eta}{1-\eta}} + c = 25.08$, which means the No.2 procurement plan in Table 4 should be applied.

¹¹Due to space limitations, the detail derivation of Equation 14 is attached in the Appendix.

¹²In warm-up period, tasks would be executed serially in order of topological sort for processing a few data in a basic cloud instance, the makespan length of tasks can be measured, then a estimated price-makespan relation table can be established by simple combination the cloud instance model and calculate the length of the critical path.

With the purchased cloud instances VM , it must satisfy the constraints of Definition 5.3 and the resource requirement can be satisfied. For convenience, we denote the number of VM as $k = |VM|$, and the CPU and GPU capacity of the i -th VM are denoted as CPU_i and GPU_i , respectively. The list of VM is sorted by their GPU capacity in descending order.

Step 3. Greedy Graph Partition. Motivated by Assumption 2, we construct a greedy graph partition strategy for minimizing the overall cost in Equation 13. This phase is towards the compounded clusters and the omisive orphaned nodes that weren't assigned into any cluster in the previous steps. Those orphaned nodes mainly include: (1) the node of an aggregation-type task demands multiple data flows produced by different GPU-intensive tasks. (2) the tasks that must be isolated due to exhaustion of computing resources of the corresponding GPU cloud server.

For each vertex (including orphaned tasks and GPU task-guided compounded clusters) in the flowline, we use objective

$$\arg \max_i \{|\mathcal{G}'_i \cap N(v')|\} \quad (16)$$

to maximize the number of neighbor nodes of vertex v' greedily, which can maximize the number of inner-partition edges and minimize the number of inter-partition edges as Equation 7. The proposed greedy graph partitioning algorithm is summarized in Algorithm 2.

Algorithm 2: Greedy Graph Partitioning

Input :Flowline $G = (V, E)$,
 Compounded tasks set $P = \{P_1, P_2, \dots, P_{|V^m|}\}$
Output:Partition strategy $\pi = \{\mathcal{G}'_1, \mathcal{G}'_2, \dots, \mathcal{G}'_k\}$

```

1  $\mathcal{G}'_{1 \rightarrow k} \leftarrow \{\emptyset\}$  // initialize partitions
2 for  $v' \in P$  do
3    $indices \leftarrow \arg \text{sort}_i \{|\mathcal{G}'_i \cap N(v')|\}$ 
4   for  $n$  of  $indices$  do
5     if  $|\mathcal{G}'_n \cap V^m| + |v' \cap V^m| \leq GPU_i$  then
6        $\mathcal{G}'_n \text{.join}(v')$ 
7       break
8   for  $v' \in \{v' | v' \in V^o \text{ and } v' \notin P\}$  do
9      $indices \leftarrow \arg \text{sort}_i \{|\mathcal{G}'_i \cap N(v')|\}$ 
10    for  $n$  of  $indices$  do
11      if  $|\mathcal{G}'_n \cap V^o| + |v' \cap V^o| \leq CPU_i - GPU_i$  then
12         $\mathcal{G}'_n \text{.join}(v')$ 
13        break

```

With the determined k size of partitions and the VM s, the computing subgraph \mathcal{G}'_i can be assigned to the corresponding VM .

Corner Case. Suppose a CPU-only flowline (e.g., the flowline is composed of operators without any deep learning model). It would skip the compounding phase. The scheduler would remain this flowline integral and purchase one VM with adequate CPUs.

Time Complexity. Algorithm 1 can substantially reduce the search space for the subsequent graph partition phase. Its complexity mainly depends on the number of GPU-intensive task $|V^m|$ and the average out-degree $|\bar{N}_{out}(V^m)|$, denotes as $O(|V^m|^2|\bar{N}_{out}(V^m)|)$. In Algorithm 2, the *argsort* procedure can be regarded as $O(k \log k)$, and the overall complexity of Algorithm 2 is $O(|V|k^2 \log k)$.

6 EXPERIMENT

6.1 End-to-end KGC Performance Evaluation

6.1.1 Experimental Setup. For the feasibility study, especially estimating the feasibility of the paradigm of serving and ensemble multiple IE models in the framework of gBuilder, we conduct experiments on various NLP tasks and benchmark datasets for evaluating the effectiveness of IE models and the performance of the whole KGC pipeline in gBuilder.

Evaluation Criteria. We use Precision (P), Recall (R), and F1 score (F) to evaluate the performance of overall triple extraction; the formulas of evaluation criteria are:

$$P = \frac{T_p}{T_p + F_p}, R = \frac{T_p}{T_p + F_n}, F = \frac{2P \cdot R}{P + R} \quad (17)$$

Where T_p denotes the number of correctly extracted triples, $T_p + F_p$ denotes the total count of the predicted triples, $T_p + F_n$ denotes the total count of gold triples which are expected to be extracted. In KGC scenario, a triple is regarded as “correct” only if its entities, relation and attribute are all exactly matched to gold standard [73].

Benchmark Datasets. We conduct experiments on four benchmark datasets in multi-language, which are all commonly used in IE research. We give a brief introduction for each dataset:

- *NYT*[61] dataset is a public IE benchmark in English. It consists of about 1M samples from New York Times articles with 24 kinds of relations. We follow the setting from Zeng et al. [79], with selected 56,195 samples for training, and 5,000 samples for validation and test, respectively.
- *WebNLG*[24] is a dataset for Natural Language Generation task and adapted for evaluating triple extraction tasks. It contains 5,019 samples for training, 500 and 703 samples for validation and testing.
- *TACRED*[86] is a large-scale relation extraction dataset in English¹³, constructed by text from newswire and web collections. It has 41 types of relations and contains 68,124 training examples and 15,509 test examples.
- *DUIE 2.0*[43] is an industrial-scale Chinese IE benchmark dataset in the general field, containing more than 11,000 training data and abundant annotation. We flatten the multiple slots schema, and only the primary object slot is regarded as the golden standard.

Models. We design 10 flowlines including joint and pipeline extraction models and then conduct KGC experiments upon them to verify the KGC performance of our system. All the IE models in flowlines are finetuned in the target dataset for a fair comparison. The details of the flowline design are described below:

(1) **Joint Models:** We employ two recent-years SOTA joint extraction models: CasRel [73] and TPLinker [70] as strong baselines, which can demonstrate the ability of our system to organize the jointly IE models.

(2) **Pipeline Models:** The pipeline models mainly consist of two stages, NER and RE, and each stage can integrate multiple models. We use the *NER*(\cdot) and *RE*(\cdot) notation to identify the task of the corresponding model. Simple operators such as filters, mappers, and integrators in the flowline are omitted. The conducted pipeline models are as follows:

¹³<https://catalog.ldc.upenn.edu/LDC2018T24>

Table 3: The experimental results of triple extraction on various benchmark datasets. \dagger marks the results are reported by original paper. $(M3)^\ddagger$ employs the RoBERTa Chinese version from Cui et al. [19].

Models	NTY			WebNLG			TACRED			DUIE2.0		
	P	R	F	P	R	F	P	R	F	P	R	F
CasRel	89.7 \dagger	89.5 \dagger	89.6 \dagger	93.4 \dagger	90.1 \dagger	91.8 \dagger	-	-	-	80.5	75.0	77.7
TPLinker	91.3 \dagger	92.5 \dagger	91.9 \dagger	91.8 \dagger	92.0 \dagger	91.9 \dagger	-	-	-	80.8	80.4	80.6
$(M1)$	69.2	65.4	67.2	72.3	72.1	72.2	59.3	61.6	60.4	68.1	66.8	67.4
$(M2)$	69.9	68.6	69.2	74.0	73.8	73.9	62.3	61.5	61.9	69.3	68.9	69.1
$(M3)$	73.7	74.3	74.0	76.1	76.3	76.2	63.8	63.6	63.7	69.9 \ddagger	70.2 \ddagger	70.0 \ddagger
$(M4)$	71.6	73.4	72.5	74.6	74.2	74.4	63.2	61.7	62.4	69.5	69.1	69.3
$(M5)$	60.4	49.2	54.2	65.2	61.6	63.3	58.9	57.5	58.2	49.8	55.1	52.3
$(M6)$	-	-	-	-	-	-	-	-	-	71.3	70.6	70.9
$(M7)$	-	-	-	-	-	-	-	-	-	73.7	74.9	74.3
$(M8)$	68.9	69.1	69.0	72.5	74.0	73.2	60.1	67.7	63.7	66.5	67.3	66.9

- $(M1)$: NER(BERT_{base}) + RE(BERT_{base})
- $(M2)$: NER(BERT_{large}) + RE(BERT_{large})
- $(M3)$: NER(RoBERTa) + RE(RoBERTa)
- $(M4)$: NER(BERT_{large}) + RE(MTB)
- $(M5)$: NER(LSTM-CRF) + RE(BiGRU-Att)
- $(M6)$: NER(FLAT) + RE(BERT_{wwm_ext})
- $(M7)$: NER(FastNER_{large}) + NER(FLAT) + RE(BERT_{wwm_ext})
- $(M8)$: NER(LSTM-CRF) + NER(BERT_{base}) + RE(BERT_{base})

Among them, BERT series models can be used to evaluate the application of PLMs in gBuilder (RoBERTa is the largest PLM among BERT series); FastNER, FLAT, and BERT_{wwm_ext} in $(M6, M7)$ are the Chinese language-specially IE models; MTB in $(M4)$ is a high-performance RE model which has a unique design and different input with other RE models; LSTM-CRF and BiGRU-Att in $(M5)$ are small models with simple structure and low-resource consumption compared with other models. The detail of models are listed in Section 4 Table 6. Through the composition and comparison of these models, the KGC performance of gBuilder can be comprehensively evaluated.

Hyper-parameters. The hyper-parameters of the deep learning model mainly include training epochs, learning rate, batch size, etc. We conducted a grid search parameter tuning experiment on the nni platform [49] for each hyper-parameter of the above models. Parameter searches were performed based on simple parameter combinations or parameters reported in the original paper. The training experiments were run for about two months on the cluster with multiple A40, V100, and P100 Nvidia Tesla cards. The possible outstanding parameter combinations will be recorded, and then perform three additional experiments based on different random seeds, and the average values will be reported as the final results.

6.1.2 Experimental Result. The experimental results are shown in Table 3. Overall, we can observe that all introduced models and flowlines organized by gBuilder (including JE models) get effective results on the four benchmark datasets, proving the capacity of gBuilder in organizing IE models for KGC, and validating the feasibility of our designed model normalization approach, model uniting and ontology merging methods.

Comparing JE models with the pipeline models, the JE model steadily outperforms the pipeline models that are composed of multiple subtask models in terms of overall performance. However, as described in Section 2, JE models have strict requirements for supervised learning data, requiring the complete annotation of the triples in the target domain dataset, which impedes the domain generalization and migration of JE, and since the benchmark datasets we employ are all customized evaluation datasets for triple extraction, that is why JE models perform well on this experiment.

Comparing different pipeline models, it is observed that the combinations composed of IE models based on PLMs $(M1-M3)$ generally achieve a better performance than the combinations of traditional models $(M5)$, and the models drawn from more extensive and advanced PLMs $(M3, M6, M7)$ tend to perform better than the base PLMs $(M1, M8)$. This phenomenon is consistent with related research [55] in the NLP community. The combination of language-specific models $(M6, M7)$ performs significantly better than other models in the corresponding language dataset, which also reveals that for language-specific KGC, linguistics features and language characteristics can be exploited to improve the effectiveness of IE models [45].

$(M7)$ adds a FastNER_{large} model than $(M6)$, which exhibits a 3.4% improvement in F1 score, and an obvious improvement (4.3 %) of recall, indicating that applying multiple models to ensemble for the subtask of IE can effectively improve the overall performance of the KGC pipeline. Comparing $(M8)$ with $(M1)$, which has an additional LSTM-CRF NER model, the recall on all 4 benchmark datasets is significantly improved (3.05% average improvement in recall value), which shows that even integrating an additional lightweight model can also help improve the recall effectiveness of large models.

These experimental results on extraction performance evaluation demonstrate the capability of the gBuilder in the organization IE models for KGC and provide insight into the design of the KGC Flowline under different circumstances.

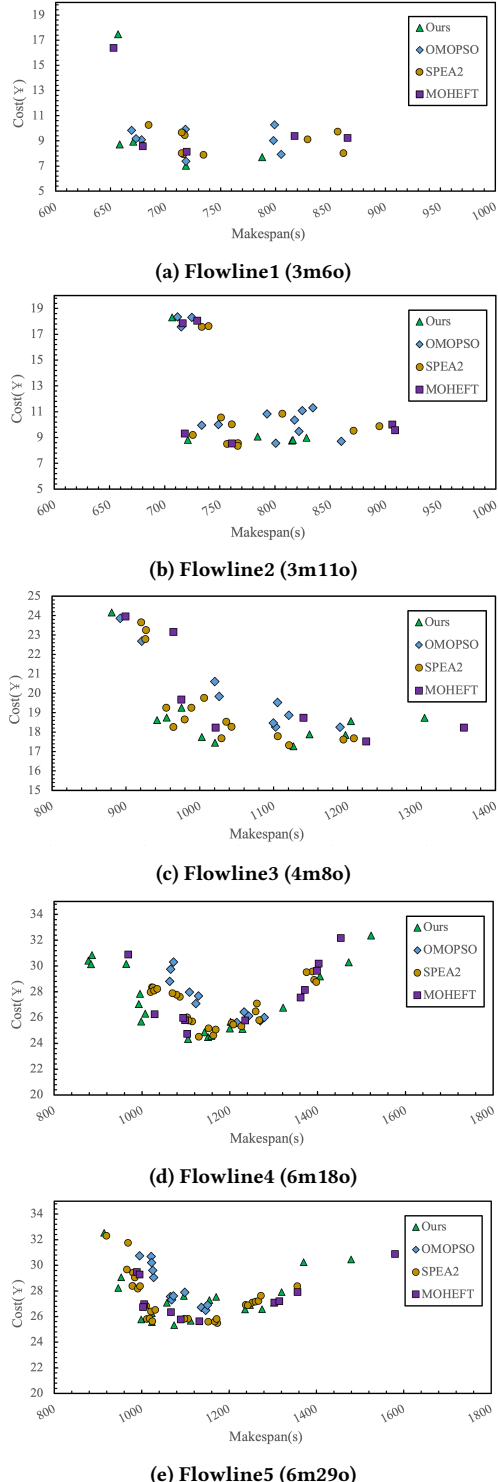


Figure 7: Monetary cost and makespan trade-offs experiments on real-world flowlines. $xm\text{yo}$ indicates the number of tasks $|V^m|$ and $|V^o|$ of the corresponding flowline.

6.2 Scheduling Evaluation

6.2.1 Experimental Setup. To verify the performance of the proposed scheduler, we organized experiments on the real-world flowlines. For evaluating the scheduling performance in the actual production environment, we collected 5 representative KGC Flowlines from beta test users and ourselves, which contains a different number of models and operators. To facilitate the measurement, we use qCloud’s GN10Xp series as the optional instances for the experiments. In order to obtain the effect of our scheduling algorithm under diversified scenarios, the η is adjustable and we try to explore as many available optimal solutions as possible, and we can observe the trade-off between makespan and monetary cost in such setting.

A subset of NYT datasets is adopted as the material to be processed by random sampling 8,000 sentences, and 200 sentences for warming up the scheduler, and employed several built-in fine-tuned models for IE (the accuracy of the IE model is not needed to consider in this evaluation). For convenience, the acquisition and termination delay of cloud instances are ignored.

Baseline Algorithms. We compare our scheduling algorithm with several baseline algorithms that target the multi-objective optimization problem [22, 81, 90], including:

- **MOHEFT**[21] developed from the famous list-based scheduling approach HEFT (Heterogeneous Earliest Finish Time), extending HEFT to address the MO problem. It is employed to optimize makespan and economic cost in cloud computing [22], and provide users with a set of optimal solutions for selecting the one that most satisfies users’ requirements.
- **SPEA2**[92] (Strength Pareto Evolutionary Algorithm) is an evolutionary algorithm that uses tournament selection to select the new population for the solution with the highest strength value. SPEA2 is often applied to explore the Pareto front for MO problems, e.g. to schedule workflow with trading-off execution time and execution price [76].
- **OMOPSO**[59] is a multi-objective Particle Swarm Optimization (PSO) algorithm to simulate the particle swarm flying through the hyper-dimensional space (search space) to explore optimal solutions. It also can be utilized to plan the MO scheduling that considers the cost and job execution time [34].

All these algorithms are implemented from open source projects [57, 58] and jMetalPy [7], and we adapt and modify those MO algorithms for scheduling. Multiple solutions generated by these baseline MO algorithms are also kept for comparison, and invalid scheduling plans (e.g., unable to meet resource requirements or the economic cost is too much higher than ours) are rejected before execution. The parameters of the algorithms keep the same as the previous works [22, 90].

6.2.2 Experimental Results. Figure 7 shows the results of scheduling experiments. Apparently, the results produced by our scheduling algorithm are significantly superior to others. Our scheduling results are leading the front of the MO optimization trade-off (closer to the lower-left corner in each subplot) compared with the baselines. That is, our algorithm for scheduling flowline can make a better solution in various scenarios that trade-off monetary cost with runtime for KGC.

The scatters tend to form multiple clusters when the number of tasks is small because different algorithms would produce the same scheduling combinations in the case of fewer tasks, resulting in close makespan and procurement costs. This trend disappears when the flowline includes more tasks because of larger *VM* clusters would introduce more randomness and perturbations such as network fluctuations. Another trend is that our algorithm constructs a much smaller number of optional combinations than other algorithms. It benefits the GPU tasks guided compounding in Algorithm 1, which reduces the search space for MO optimization.

These scheduling experiments demonstrate that our proposed scheduling algorithm for gBuilder can effectively schedule tasks in KGC (including IE models and operators, etc.) and outperforms the benchmark algorithms like MOHEFT, SPEA2, and OMOPSO.

7 CONCLUSION

This paper presents gBuilder, a high usability and scalability KGC system for extracting structured knowledge instances from the unstructured corpus by organizing multiple operators and IE models. Compared with existing KGC systems and distributed computing systems, gBuilder combines their strengths, enabling flexible large-scale KGC through greedy graph partitioning scheduling algorithms over the proposed concept of flowline, which is an abstract of IE workflow and data pipeline. Extensive end-to-end knowledge extraction experiments and scheduling experiments demonstrate the usability and scalability of our proposed system. An extensive beta test and user feedback also show the usefulness of our system in KGC applications.

REFERENCES

- [1] Bilal Abu-Salih. 2021. Domain-specific knowledge graphs: A survey. *Journal of Network and Computer Applications* 185 (2021), 103076.
- [2] Raghu Anantharangachar, Srinivasan Ramani, and S Rajagopalan. 2013. Ontology guided information extraction from unstructured text. *arXiv preprint arXiv:1302.1335* (2013).
- [3] Muhammad Nabeel Asim, Muhammad Wasim, Muhammad Usman Ghani Khan, Waqar Mahmood, and Hafiza Mahnoor Abbasi. 2018. A survey of ontology learning techniques and applications. *Database* 2018 (2018).
- [4] Sören Auer, Christian Bizer, Georgi Kobilarov, Jens Lehmann, Richard Cyganiak, and Zachary Ives. 2007. Dbpedia: A nucleus for a web of open data. In *The semantic web*. Springer, 722–735.
- [5] Livio Baldini Soares, Nicholas FitzGerald, Jeffrey Ling, and Tom Kwiatkowski. 2019. Matching the Blanks: Distributional Similarity for Relation Learning. In *Proceedings of the 57th Annual Meeting of the Association for Computational Linguistics*. Association for Computational Linguistics, Florence, Italy, 2895–2905. <https://doi.org/10.18653/v1/P19-1279>
- [6] Livio Baldini Soares, Nicholas FitzGerald, Jeffrey Ling, and Tom Kwiatkowski. 2019. Matching the Blanks: Distributional Similarity for Relation Learning. In *Proceedings of the 57th Annual Meeting of the Association for Computational Linguistics*. Association for Computational Linguistics, Florence, Italy, 2895–2905. <https://doi.org/10.18653/v1/P19-1279>
- [7] Antonio Benítez-Hidalgo, Antonio J. Nebro, José García-Nieto, Izaskun Oregi, and Javier Del Ser. 2019. jMetalPy: A Python framework for multi-objective optimization with metaheuristics. *Swarm and Evolutionary Computation* (2019), 100598. <https://doi.org/10.1016/j.swevo.2019.100598>
- [8] Chris Biemann. 2005. Ontology learning from text: A survey of methods.. In *LDV forum*, Vol. 20. 75–93.
- [9] Kurt Bollacker, Colin Evans, Praveen Paritosh, Tim Sturge, and Jamie Taylor. 2008. Freebase: a collaboratively created graph database for structuring human knowledge. In *Proceedings of the 2008 ACM SIGMOD international conference on Management of data*. 1247–1250.
- [10] J. Bruno, E. G. Coffman, and R. Sethi. 1974. Scheduling Independent Tasks to Reduce Mean Finishing Time. *Commun. ACM* 17, 7 (jul 1974), 382–387. <https://doi.org/10.1145/361011.361064>
- [11] Per Nikolaj D Buhk. 1992. The art of computer systems performance analysis, techniques for experimental design, measurement, simulation and modeling.
- [12] Qingxing Cao and Bo Zhao. 2020. Application of Open-Source Software in Knowledge Graph Construction. *e-Learning, e-Education, and Online Training* 340 (2020), 97 – 102.
- [13] Paris Carbone, Asterios Katsifodimos, Stephan Ewen, Volker Markl, Seif Haridi, and Kostas Tzoumas. 2015. Apache flink: Stream and batch processing in a single engine. *Bulletin of the IEEE Computer Society Technical Committee on Data Engineering* 36, 4 (2015).
- [14] Kathleen Carley. 1988. Formalizing the social expert's knowledge. *Sociological Methods & Research* 17, 2 (1988), 165–232.
- [15] Asli Celikyilmaz and Dilek Hakkan-Tur. 2015. Investigation of ensemble models for sequence learning. In *2015 IEEE International Conference on Acoustics, Speech and Signal Processing (ICASSP)*. IEEE, 5381–5385.
- [16] Chia-Hui Chang, Mohammed Kayed, Moheb R Giris, and Khaled F Shaalan. 2006. A survey of web information extraction systems. *IEEE transactions on knowledge and data engineering* 18, 10 (2006), 1411–1428.
- [17] Xiaojun Chen, Shengbin Jia, and Yang Xiang. 2020. A review: Knowledge reasoning over knowledge graph. *Expert Systems with Applications* 141 (2020), 112948.
- [18] Sharan Chetlur, Cliff Woolley, Philippe Vandermersch, Jonathan Cohen, John Tran, Bryan Catanzaro, and Evan Shelhamer. 2014. cudnn: Efficient primitives for deep learning. *arXiv preprint arXiv:1410.0759* (2014).
- [19] Yiming Cui, Wanxiang Che, Ting Liu, Bing Qin, and Ziqing Yang. 2021. Pre-Training with Whole Word Masking for Chinese BERT. <https://doi.org/10.1109/TASLP.2021.3124365>
- [20] Jacob Devlin, Ming-Wei Chang, Kenton Lee, and Kristina Toutanova. 2019. BERT: Pre-training of Deep Bidirectional Transformers for Language Understanding. In *Proceedings of the 2019 Conference of the North American Chapter of the Association for Computational Linguistics: Human Language Technologies, Volume 1 (Long and Short Papers)*. Association for Computational Linguistics, Minneapolis, Minnesota, 4171–4186. <https://doi.org/10.18653/v1/N19-1423>
- [21] Juan José Durillo, Hamid Mohammadi Fard, and Radu Prodan. 2012. MOHEFT: A multi-objective list-based method for workflow scheduling. *4th IEEE International Conference on Cloud Computing Technology and Science Proceedings* (2012), 185–192.
- [22] Juan J Durillo and Radu Prodan. 2014. Multi-objective workflow scheduling in Amazon EC2. *Cluster computing* 17, 2 (2014), 169–189.
- [23] Dieter Fensel, Umutcan Şimşek, Kevin Angele, Elwin Huaman, Elias Kärle, Oleksandra Panasiuk, Ioan Toma, Jürgen Umbrich, and Alexander Wahler. 2020. *Introduction: What Is a Knowledge Graph?* Springer International Publishing, Cham, 1–10. https://doi.org/10.1007/978-3-030-37439-6_1
- [24] Claire Gardent, Anastasia Shimorina, Shashi Narayan, and Laura Perez-Beltrachini. 2017. Creating Training Corpora for NLG Micro-Planners. In *Proceedings of the 55th Annual Meeting of the Association for Computational Linguistics, ACL 2017, Vancouver, Canada, July 30 - August 4, Volume 1: Long Papers*, Regina Barzilay and Min-Yen Kan (Eds.). Association for Computational Linguistics, 179–188. <https://doi.org/10.18653/v1/P17-1017>
- [25] Michael R Garey and David S Johnson. 1979. *Computers and intractability*. Vol. 174. freeman San Francisco.
- [26] Zhichao Geng, Hang Yan, Xipeng Qiu, and Xuanjing Huang. 2021. fastHan: A BERT-based Multi-Task Toolkit for Chinese NLP. In *Proceedings of the 59th Annual Meeting of the Association for Computational Linguistics and the 11th International Joint Conference on Natural Language Processing: System Demonstrations*. 99–106. <https://aclanthology.org/2021.acl-demo-12>
- [27] Juncheng Gu, Mosharaf Chowdhury, Kang G Shin, Yibo Zhu, Myeongjae Jeon, Junjie Qian, Hongqiang Liu, and Chuanxiong Guo. 2019. Tiresias: A {GPU} cluster manager for distributed deep learning. In *16th USENIX Symposium on Networked Systems Design and Implementation (NSDI 19)*. 485–500.
- [28] Qingyu Guo, Fuzhen Zhuang, Chuan Qin, Hengshu Zhu, Xing Xie, Hui Xiong, and Qing He. 2020. A survey on knowledge graph-based recommender systems. *IEEE Transactions on Knowledge and Data Engineering* (2020).
- [29] P Hitzler, M Krotzsch, M Ehrig, and Y Sure. 2005. What is ontology merging?—a categorytheoretical perspective using pushouts. American Association of Artificial Intelligence.
- [30] Johannes Hoffart, Fabian M Suchanek, Klaus Berberich, and Gerhard Weikum. 2013. YAGO2: A spatially and temporally enhanced knowledge base from Wikipedia. *Artificial intelligence* 194 (2013), 28–61.
- [31] Sen Hu, Lei Zou, Jeffrey Xu Yu, Haixun Wang, and Dongyan Zhao. 2017. Answering natural language questions by subgraph matching over knowledge graphs. *IEEE Transactions on Knowledge and Data Engineering* 30, 5 (2017), 824–837.
- [32] Yimin Jiang, Yibo Zhu, Chang Lan, Bairén Yi, Yong Cui, and Chuanxiong Guo. 2020. A Unified Architecture for Accelerating Distributed {DNN} Training in Heterogeneous {GPU/CPU} Clusters. In *14th USENIX Symposium on Operating Systems Design and Implementation (OSDI 20)*. 463–479.
- [33] Yannis Kalfoglou and Marco Schorlemmer. 2002. Information-flow-based ontology mapping. In *OTM Confederated International Conferences "On the Move to Meaningful Internet Systems"*. Springer, 1132–1151.
- [34] Mandeep Kaur and Sanjay Kadam. 2018. A novel multi-objective bacteria foraging optimization algorithm (MOBFOA) for multi-objective scheduling. *Applied Soft*

Computing 66 (2018), 183–195.

[35] Mayank Kejriwal. 2019. *Domain-specific knowledge graph construction*. Springer.

[36] Nathawut Kertkeekachorn and Ryutaro Ichise. 2017. T2kg: An end-to-end system for creating knowledge graph from unstructured text. In *Workshops at the Thirty-First AAAI Conference on Artificial Intelligence*.

[37] Muhammad Khan, Ali Imran Jehangiri, Zulfiqar Ahmad, Mohammed Alaa Ala'anzy, and Asif Umer. 2022. An exploration to graphics processing unit spot price prediction. *Cluster Computing* (2022), 1–17.

[38] Sarath Kumar Kondreddi, Peter Triaftafillou, and Gerhard Weikum. 2014. Combining information extraction and human computing for crowdsourced knowledge acquisition. In *2014 IEEE 30th International Conference on Data Engineering*. IEEE, 988–999.

[39] Shantanu Kumar. 2017. A survey of deep learning methods for relation extraction. *arXiv preprint arXiv:1705.03645* (2017).

[40] Krzysztof Kurowski, Jarek Nabrzyski, Ariel Oleksiak, and Jan Weglarz. 2006. Grid multicriteria job scheduling with resource reservation and prediction mechanisms. In *Perspectives in modern project scheduling*. Springer, 345–373.

[41] Chang-Shing Lee, Yuan-Fang Kao, Yau-Hwang Kuo, and Mei-Hui Wang. 2007. Automated ontology construction for unstructured text documents. *Data & Knowledge Engineering* 60, 3 (2007), 547–566.

[42] Jing Li, Aixin Sun, Jianglei Han, and Chenliang Li. 2020. A survey on deep learning for named entity recognition. *IEEE Transactions on Knowledge and Data Engineering* (2020).

[43] Shuangjie Li, Wei He, Yabing Shi, Wenbin Jiang, Haijin Liang, Ye Jiang, Yang Zhang, Jayaun Lyu, and Yong Zhu. 2019. Duie: A large-scale chinese dataset for information extraction. In *CCF International Conference on Natural Language Processing and Chinese Computing*. Springer, 791–800.

[44] Xiaonan Li, Hang Yan, Xipeng Qiu, and Xuanjing Huang. 2020. FLAT: Chinese NER Using Flat-Lattice Transformer. In *Proceedings of the 58th Annual Meeting of the Association for Computational Linguistics*. Association for Computational Linguistics, Online, 6836–6842. <https://doi.org/10.18653/v1/2020.acl-main.611>

[45] Yanzeng Li, Jiangxia Cao, Xin Cong, Zhenyu Zhang, Bowen Yu, Hongsong Zhu, and Tingwen Liu. 2022. Enhancing Chinese Pre-trained Language Model via Heterogeneous Linguistics Graph. In *Proceedings of the 60th Annual Meeting of the Association for Computational Linguistics (Volume 1: Long Papers)*. Association for Computational Linguistics, Dublin, Ireland, 1986–1996. <https://doi.org/10.18653/v1/2022.acl-long.140>

[46] Weijie Liu, Peng Zhou, Zhe Zhao, Zhiruo Wang, Qi Ju, Haotang Deng, and Ping Wang. 2020. K-bert: Enabling language representation with knowledge graph. In *Proceedings of the AAAI Conference on Artificial Intelligence*, Vol. 34. 2901–2908.

[47] Jose L Martinez-Rodriguez, Aidan Hogan, and Ivan Lopez-Arevalo. 2020. Information extraction meets the semantic web: a survey. *Semantic Web* 11, 2 (2020), 255–335.

[48] Paul McGuire. 2007. *Getting started with pyparsing*. "O'Reilly Media, Inc".

[49] Microsoft. 2022. *Neural Network Intelligence*. <https://github.com/microsoft/nni>

[50] Ajinkya More. 2016. Attribute extraction from product titles in ecommerce. *arXiv preprint arXiv:1608.04670* (2016).

[51] Mark A Musen. 2015. The protégé project: a look back and a look forward. *AI matters* 1, 4 (2015), 4–12.

[52] David Nadeau and Satoshi Sekine. 2007. A survey of named entity recognition and classification. *Lingvisticae Investigationes* 30, 1 (2007), 3–26.

[53] Alberto Paccanaro and Geoffrey E. Hinton. 2001. Learning distributed representations of concepts using linear relational embedding. *IEEE Transactions on Knowledge and Data Engineering* 13, 2 (2001), 232–244.

[54] Gustavo Portella, Genaina N Rodrigues, Eduardo Nakano, and Alba CMA Melo. 2019. Statistical analysis of Amazon EC2 cloud pricing models. *Concurrency and Computation: Practice and Experience* 31, 18 (2019), e4451.

[55] Xipeng Qiu, Tianxiang Sun, Yige Xu, Yunfan Shao, Ning Dai, and Xuanjing Huang. 2020. Pre-trained models for natural language processing: A survey. *Science China Technological Sciences* 63, 10 (2020), 1872–1897.

[56] Alec Radford, Karthik Narasimhan, Tim Salimans, and Ilya Sutskever. 2018. Improving language understanding with unsupervised learning. (2018).

[57] Online Repo. 2017. MO Scheduling. <https://github.com/leimiaomiao/Multi-Objective-Workflow-Scheduling>.

[58] Online Repo. 2021. Intelligent Algorithm Scheduler. <https://github.com/ZhaoKe1024/IntelligentAlgorithmScheduler>.

[59] M. Reyes and C.A. Coello Coello. 2005. Improving PSO-based Multi-objective Optimization Using Crowding, Mutation and ϵ -dominance. In *Third International Conference on Evolutionary MultiCriterion Optimization, EMO 2005 (LNCS)*, C.A. Coello, A. Hernández, and E. Zitzler (Eds.), Vol. 3410. Springer, 509–519.

[60] Ian Robinson, Jim Webber, and Emil Eifrem. 2015. *Graph databases: new opportunities for connected data*. "O'Reilly Media, Inc".

[61] Evan Sandhaus. 2008. The new york times annotated corpus. *Linguistic Data Consortium, Philadelphia* 6, 12 (2008), e26752.

[62] Cristina Sarasua, Elena Simperl, Natasha F Noy, Abraham Bernstein, and Jan Marco Leimeister. 2015. Crowdsourcing and the semantic web: A research manifesto. *Human Computation* 2, 1 (2015).

[63] Heiner Stuckenschmidt. 2002. Approximate information filtering on the semantic web. In *Annual Conference on Artificial Intelligence*. Springer, 114–128.

[64] Sen Su, Jian Li, Qingjia Huang, Xiao Huang, Kai Shuang, and Jie Wang. 2013. Cost-efficient task scheduling for executing large programs in the cloud. *Parallel Comput.* 39, 4–5 (2013), 177–188.

[65] Erik F. Tjong Kim Sang and Fien De Meulder. 2003. Introduction to the CoNLL-2003 Shared Task: Language-Independent Named Entity Recognition. In *Proceedings of the Seventh Conference on Natural Language Learning at HLT-NAACL 2003*. 142–147. <https://aclanthology.org/W03-0419>

[66] Christina Unger, Lorenz Bühmann, Jens Lehmann, Axel-Cyrille Ngonga Ngomo, Daniel Gerber, and Philipp Cimiano. 2012. Template-based question answering over RDF data. In *Proceedings of the 21st international conference on World Wide Web*. 639–648.

[67] Damir Vandic, Jan-Willem Van Dam, and Flavius Frasincar. 2012. Faceted product search powered by the Semantic Web. *Decision Support Systems* 53, 3 (2012), 425–437.

[68] Chengbin Wang, Xiaogang Ma, Jianguo Chen, and Jingwen Chen. 2018. Information extraction and knowledge graph construction from geoscience literature. *Computers & geosciences* 112 (2018), 112–120.

[69] Haitao Wang, Zhengqiu He, Jin Ma, Wenliang Chen, and Min Zhang. 2019. Ippe: a dataset for inter-personal relationship extraction. In *CCF International Conference on Natural Language Processing and Chinese Computing*. Springer, 103–115.

[70] Yucheng Wang, Bowen Yu, Yueyang Zhang, Tingwen Liu, Hongsong Zhu, and Limin Sun. 2020. TPLinker: Single-stage Joint Extraction of Entities and Relations Through Token Pair Linking. In *Proceedings of the 28th International Conference on Computational Linguistics*. International Committee on Computational Linguistics, Barcelona, Spain (Online), 1572–1582. <https://www.aclweb.org/anthology/2020.coling-main.138>

[71] James Warren and Nathan Marz. 2015. *Big Data: Principles and best practices of scalable realtime data systems*. Simon and Schuster.

[72] Zhepei Wei, Jianlin Su, Yue Wang, Yuan Tian, and Yi Chang. 2020. A Novel Cascade Binary Tagging Framework for Relational Triple Extraction. In *Proceedings of the 58th Annual Meeting of the Association for Computational Linguistics*. Association for Computational Linguistics, Online, 1476–1488. <https://doi.org/10.18653/v1/2020.acl-main.136>

[73] Zhepei Wei, Jianlin Su, Yue Wang, Yuan Tian, and Yi Chang. 2020. A Novel Cascade Binary Tagging Framework for Relational Triple Extraction. In *Proceedings of the 58th Annual Meeting of the Association for Computational Linguistics*. 1476–1488.

[74] Kevin Wilkinson and Kevin Wilkinson. 2006. Jena property table implementation.

[75] Zhilin Yang, Zihang Dai, Yiming Yang, Jaime G. Carbonell, Ruslan Salakhutdinov, and Quoc V. Le. 2019. XLNet: Generalized Autoregressive Pretraining for Language Understanding. In *Advances in Neural Information Processing Systems 32: Annual Conference on Neural Information Processing Systems 2019, NeurIPS 2019, December 8–14, 2019, Vancouver, BC, Canada*, Hanna M. Wallach, Hugo Larochelle, Alina Beygelzimer, Florence d'Alché-Buc, Emily B. Fox, and Roman Garnett (Eds.), 5754–5764. <https://proceedings.neurips.cc/paper/2019/hash/dc6a7e655d7e5840e66733e9ee67cc69-Abstract.html>

[76] Jia Yu, Michael Kirley, and Rajkumar Buyya. 2007. Multi-objective planning for workflow execution on grids. In *2007 8th IEEE/ACM International Conference on Grid Computing*. IEEE, 10–17.

[77] Matei Zaharia, Reynold S Xin, Patrick Wendell, Tathagata Das, Michael Armbrust, Ankur Dave, Xiangrui Meng, Josh Rosen, Shivaram Venkataraman, Michael J Franklin, et al. 2016. Apache spark: a unified engine for big data processing. *Commun. ACM* 59, 11 (2016), 56–65.

[78] Matei Zaharia, Reynold S Xin, Patrick Wendell, Tathagata Das, Michael Armbrust, Ankur Dave, Xiangrui Meng, Josh Rosen, Shivaram Venkataraman, Michael J Franklin, et al. 2016. Apache spark: a unified engine for big data processing. *Commun. ACM* 59, 11 (2016), 56–65.

[79] Xiangrong Zeng, Daojian Zeng, Shizhu He, Kang Liu, and Jun Zhao. 2018. Extracting relational facts by an end-to-end neural model with copy mechanism. In *Proceedings of the 56th Annual Meeting of the Association for Computational Linguistics (Volume 1: Long Papers)*. 506–514.

[80] Ce Zhang. 2015. *DeepDive: a data management system for automatic knowledge base construction*. Ph.D. Dissertation. The University of Wisconsin-Madison.

[81] Fan Zhang, Junwei Cao, Kebin Li, Samee U Khan, and Kai Hwang. 2014. Multi-objective scheduling of many tasks in cloud platforms. *Future Generation Computer Systems* 37 (2014), 309–320.

[82] Li Zhang, Yanzeng Li, Rouyu Zhang, and Wenjie Li. 2021. Semi-Open Attribute Extraction from Chinese Functional Description Text. In *Asian Conference on Machine Learning*. PMLR, 1505–1520.

[83] Minhao Zhang, Ruoya Zhang, Yanzeng Li, and Lei Zou. 2022. Crake: Causal-Enhanced Table-Filler for Question Answering over Large Scale Knowledge Base. In *Proceedings of the 2022 Annual Conference of the North American Chapter of the Association for Computational Linguistics*.

[84] Ningyu Zhang, Xin Xu, Liankuan Tao, Haiyang Yu, Hongbin Ye, Xin Xie, Xiang Chen, Zhoubo Li, Lei Li, Xiaozhuan Liang, Yunzhi Yao, Shumin Deng, Wen

Zhang, Zhenru Zhang, Chuanqi Tan, Fei Huang, Guozhou Zheng, and Huajun Chen. 2022. DeepKE: A Deep Learning Based Knowledge Extraction Toolkit for Knowledge Base Population. <https://doi.org/10.48550/ARXIV.2201.03335>

[85] Yue Zhang and Jie Yang. 2018. Chinese NER Using Lattice LSTM. In *Proceedings of the 56th Annual Meeting of the Association for Computational Linguistics (Volume 1: Long Papers)*. Association for Computational Linguistics, Melbourne, Australia, 1554–1564. <https://doi.org/10.18653/v1/P18-1144>

[86] Yuhao Zhang, Victor Zhong, Danqi Chen, Gabor Angeli, and Christopher D. Manning. 2017. Position-aware Attention and Supervised Data Improve Slot Filling. In *Proceedings of the 2017 Conference on Empirical Methods in Natural Language Processing (EMNLP 2017)*. 35–45. <https://nlp.stanford.edu/pubs/zhang2017tacred.pdf>

[87] Zhengyan Zhang, Xu Han, Zhiyuan Liu, Xin Jiang, Maosong Sun, and Qun Liu. 2019. ERNIE: Enhanced language representation with informative entities. *arXiv preprint arXiv:1905.07129* (2019).

[88] Xuejiao Zhao, Zhenchang Xing, Muhammad Ashad Kabir, Naoya Sawada, Jing Li, and Shang-Wei Lin. 2017. Hdskg: Harvesting domain specific knowledge graph from content of webpages. In *2017 ieee 24th international conference on software analysis, evolution and reengineering (saner)*. IEEE, 56–67.

[89] Zhanfang Zhao, Sung-Kook Han, and In-Mi So. 2018. Architecture of knowledge graph construction techniques. *International Journal of Pure and Applied Mathematics* 118, 19 (2018), 1869–1883.

[90] Xiumin Zhou, Gongxuan Zhang, Jin Sun, Junlong Zhou, Tongquan Wei, and Shiyuan Hu. 2019. Minimizing cost and makespan for workflow scheduling in cloud using fuzzy dominance sort based HEFT. *Future Generation Computer Systems* 93 (2019), 278–289.

[91] Zhi-Hua Zhou. 2021. Ensemble learning. In *Machine learning*. Springer, 181–210.

[92] Eckart Zitzler, Marco Laumanns, and Lothar Thiele. 2002. SPEA2: Improving the Strength Pareto Evolutionary Algorithm For Multiobjective Optimization.

[93] Lei Zou, M. Tamer Özsu, Lei Chen, Xuchuan Shen, Ruizhe Huang, and Dongyan Zhao. 2013. gStore: a graph-based SPARQL query engine. *The VLDB Journal* 23 (2013), 565–590.

[94] Xiaohan Zou. 2020. A survey on application of knowledge graph. In *Journal of Physics: Conference Series*, Vol. 1487. IOP Publishing, 012016.

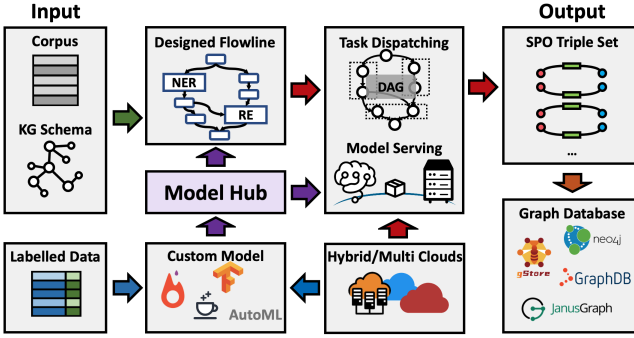


Figure 8: The overview diagram of gBuilder.

A SYSTEM ARCHITECTURE

gBuilder is proposed to construct KGs from large-scale unstructured text. It is modularly developed following the microservices architecture and supports concurrent KGC for multiple projects and multi-users. Furthermore, gBuilder deploys in multi-cloud environments to scale-up computing resources at cloud providers to dynamically meet the requirements of large-scale KGC. This section introduces the architecture of gBuilder functionally.

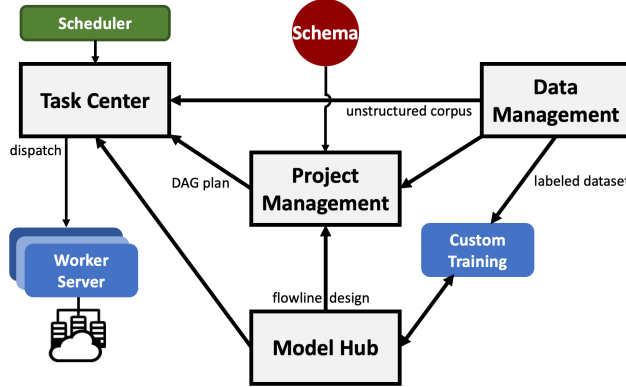


Figure 9: The architecture of gBuilder.

A.1 Modules

As Figure 9 shows, gBuilder is composed of four main modules.

Project Management module is the core component of gBuilder. It controls the entire KBC process, including Flowline-related features (design, storage, verify), user authentication, logging collector, etc. This module also schedules other modules through inter-services communication and manages the KGC workflow from import of schema to generation of DAG execution plan.

Data Management module manages the corpora of the project, including unstructured corpus for inference and labeled data for training. This module is the data source of KGC. It will divide the data by column or row according to the needs of the task center and push the data slice to the specified service.

Model Hub manages all deep learning models in gBuilder, including built-in models and custom models. When a task calls for

a well-tuned IE model, the model hub will transfer the skeleton and weights of a model to the corresponding worker node and instantiate it on the worker server. In addition, the model hub also controls the training process of custom models, including applying computing resources, controlling hyperparameters tuning, etc. We also provide an interface to accept user-custom model endpoints to contain users' self-server models or algorithms in Model Hub and insert into the KGC flowline.

Task Center controls the scheduling of tasks. This module will further divide the DAG execution plan obtained from the project management module, and find out the parallel and serial relation in the DAG. The isolative sequence of tasks that can be executed independently will be integrated as one job. Then the task center will apply and assign computing resources on demand for each job. The operator and task-related data corresponding to the job will be instantiated on the terminal node. Besides, the task center also collects generated loggings, and monitors the execution status of each node and the transmission of data.

Besides the four main modules of the core service, **Worker Server** is also an essential part of gBuilder. It is the service that instantiates on the terminal computing node, executes the job according to the schedule from the task center, instantiates the IE model transmitted from the Model Hub, obtains input data from the predecessor tasks, and preprocesses output data for the successor tasks.

B USER INTERFACES

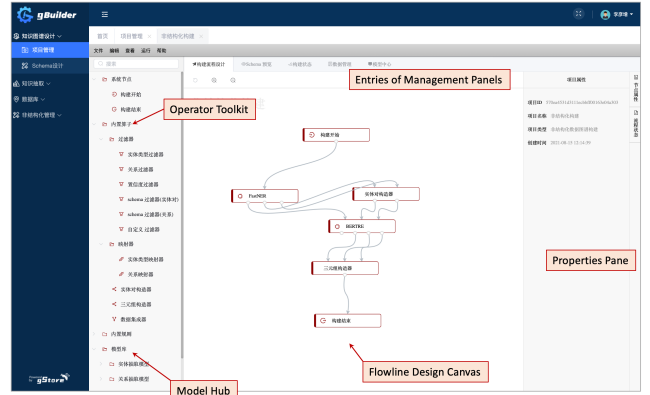


Figure 10: The main interface (including flowline canvas) of gBuilder.

C GRAPHIC FLOWLINE LANGUAGE

Graphic Flowline Language (GFL) is a plain DSL for formally defining the Flowline, implemented by pyparsing[48]. Listing 1 is equivalent to Flowline Exp1 (Figure 5), it shows the basic syntax of GFL. `:=` denotes variable definitions, `:` denotes the unique entry and output of the Flowline, `|` denotes the data pipe within Flowline. Functions like BertNER, filter are the built-in or user-imported operators or IE models, the values in the followed square brackets `[.]` are the corresponding function name (optional) for distinguishing between different calls to the same operator, the values in the

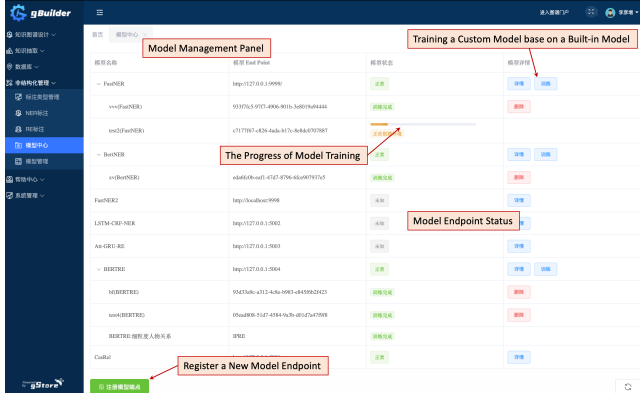


Figure 11: The model management interface.

```

filtered_ent := []
:data
  | model.BertNER -> ent, ent_t
  | opt.filter[f_bert](ent_t in filtered_ent)
  | opt.permute[p1] -> ent_p, ent_t_p
  | model.BERTRE -> rel, ent_p, ent_t_p
  | opt.filter[f_lstm](ent_t not in filtered_ent)
  | opt.permute[p2] -> ent_p, ent_t_p
  | model.LSTMRE -> rel, ent_p, ent_t_p
  | model.BERTRE
  | opt.merge[re]
  | model.LSTMRE
  | opt.merge[re]
  | opt.triple:

```

Listing 1: Abstract syntax for GFL

followed parentheses (.) are the definition of lambda expression for the corresponding function. Python-like indent is employed for deciding the scope and the connection of Flowline. With GFL, expert users can conveniently define their knowledge graph construction process formally and use lambda/regular expressions to design a more flexible Flowline. The visual interaction Flowline design in gBuilder is interconvertible with GFL.

D HARDNESS ANALYSIS

We provide a simple proof for hardness of Theorem 5.4.

PROOF. Considering with a special case with $\eta = 1$, which means only the $cost_{com}$ would be considered. In this case, the DAG partitioning problem equals to the Minimum Makespan Scheduling problem [25] with $|V|$ jobs and k machines, which has been proven that the Minimum Makespan Scheduling problem has no polynomial-time approximation algorithm with a finite approximation factor unless $P = NP$ if $k > 1$ [10]. Therefore, the theorem holds. \square

E MINIMUM MAKESPAN ESTIMATION VIA PROCUREMENT PRICING

For convenience, we employ $P(G)$ to denote the unit monetary cost for purchasing VMs with enough capacity to contain the flowline G , as $\sum_{i=1}^{i=k} Price(v_{mi})$ in Equation 10 in the reality cloud market. Since price is related to the infrastructure cost of cloud vendors (including hardware, electricity, etc.), which are meditately related to the

computing power (e.g., FLOPS) and affect the length of makespan, we hypothetically define a function $M(G) = g(P(G))$ to model the relation between price and makespan. For convenience, we denote it as $y = g(x)$, the function g satisfies the follow properties:

- Domain of g is $x > 0$ and range of g is $y > 0$;
- $\lim_{x \rightarrow +\infty} g(x) = a$, where a is a constant. With a given G , suppose ideally that we can purchase a powerful enough VM that meets the resources constraint with monolithic-machine performance, and all the tasks (including IE models and operators) can run on this VM asynchronously and concurrently. Under this condition, the scheduling achieves the optimal performance $cost_{com} \propto M(G)$, the makespan $M(G)$ is equivalent to the critical path of weighted DAG G and is impossible to make a shorter $M(G)$ even with unlimited pricing.
- $\lim_{x \rightarrow 0^+} g(x) = +\infty$. Suppose we don't want to spend much money on purchasing VMs, the procurement plan will tend to purchase multiple small-capacity VMs, which will also cause the flowline to be partitioned excessively, resulting in huge communication overhead. In the extreme case, our procurement fund is not enough to meet the resource requirement of the execution of the flowline, which will lead to an infinite makespan $M(G)$.
- $g(x_1) \geq g(x_2), x_1 < x_2$. According to common sense, large $P(G)$ would purchase more computing power and reducing makespan $M(G)$ naturally, as (x_3, y_3) and (x_1, y_1) in Figure 12a (a). However, in distributed computing scenarios, we should also consider the situation after partitioning. Assuming makespan $M(G)$ only depends on CPU and GPU resources: execution of flowline G requires A CPUs and B GPUs. With partitioning G into 2 clusters, suppose one of the sub-clusters requires a CPUs and b GPUs, according to Equation 10, $Price(A, B) = Price(a, b) + Price(A - a, B - b)$. Nevertheless, we generally purchase VMs with sufficient GPUs but superfluous CPUs: $Price(A, B) \leq Price(ar, b) + Price(C, B - b)$, where $ar \leq a$ and $C \leq A - a$, and it is equivalent to

$$P(G) \leq P(G') \quad (18)$$

For the partitioned G , there are generally $M(G) \leq M(G')$, and the increment is mainly due to the increased communication cross VMs. This status is described as (x_1, y_1) and (x_1, y_2) in Figure 12a (a).

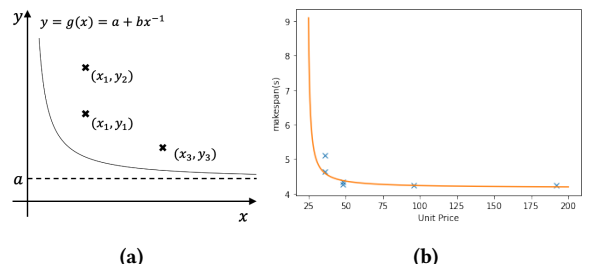


Figure 12: (a) The hypothetical dominant function between $P(G)$ to $M(G)$. (b) The visual scatterplot of Table 5 and the boundary curve of Equation 19 under the fitted coefficients ($a = 4.17$, $b = 5.15$, $c = 23.96$).

We define a simple polynomial function

$$y = a + b(x - c)^{-1}, (a, b, c, x > 0) \quad (19)$$

to model g as Figure 12a, which describes the front of $P(G)$ and $M(G)$. For testing this model in the real world data, we conduct verification experiment on qCloud(Tencent Cloud¹⁴), which is an IaaS cloud computing platform provided by Tencent Holdings Ltd. The configuration and price (pay-as-you-go billing model) of GPU instance of qCloud’s GN10Xp series¹⁵ are listed in Table 4. We employ cloud instances from the above products for estimating

Table 4: Instance model configuration and pricing of qCloud GN10Xp family.

Instance	GPU num	GPU memory	CPU cores	Memory size	Unit Price (per hour)
2XLARGE40	1	32	10	40	¥11.98
5XLARGE80	2	64	20	80	¥23.96
10XLARGE160	4	128	40	160	¥47.92
20XLARGE320	8	256	80	320	¥95.84

the relationship between makespan and pricing. The pre-defined flowline as Figure 5 is introduced as the workload, and the scheduler algorithm proposed in this paper is applied for scheduling. We conducted the experiment 5 times and reported the average value. The results are shown in Table 5. The No.0 procurement plan

Table 5: Price and makespan for executing example Flowline (as Figure 5) in real-world. The bolded “(·)X” denotes the corresponding instance model “(·)XLARGE” in Table 4.

No.	VM group	Makespan(s)	Total Price (¥)	Unit Price (¥)
0	2X × 2	∞	-	23.96
1	2X × 3	5.10	0.050	35.94
2	5X × 1 + 2X × 1	4.65	0.046	35.94
3	5X × 2	4.34	0.058	47.92
4	10X × 1	4.26	0.056	47.92
5	20X × 1	4.25	0.113	95.84
6	20X × 2	4.25	0.226	191.68

(#GPU < |V^m|) does not satisfy the requirement of resources that would commit an unacceptable makespan length. Using non-linear least squares to fit the boundary curve of scatters would produce $a = 4.17$, $b = 5.15$ and $c = 23.96$, as Figure 12b shows.

Substituting the hypothesis polynomial function relationship between price and makespan into the objective function, it can be rewritten as:

$$J = f(x) = \eta g(x) + (1 - \eta)x \cdot g(x) \quad (20)$$

which is a convex function with a global minimum at $x_0 = \sqrt{\frac{b}{a}} \frac{\eta}{1-\eta} + c$, and our objective target is to approach the minimum as possible (Since the procurement plan of VMs is discrete, it is unpractical to

¹⁴<https://intl.cloud.tencent.com>

¹⁵<https://intl.cloud.tencent.com/document/product/560/19701#GN10Xp>

close x_0 continuously). The value of constants a and b depend on the cloud vendors, and weight of η is determined by user¹⁶.

F BUILT-IN MODELS

gBuilder provides a “matrix” of built-in models which have different model structure and pre-trained in different datasets.

Table 6: Part of the built-in IE models. †indicates the model is implemented from the original paper author. ‡indicates the model is implemented from the open-source project. * indicates the model is implemented by ourselves.

Type	id	Model	Source
NER	1	FastNER _{base}	Geng et al. [26]†‡
	2	FastNER _{large}	Geng et al. [26]†‡
	3	LSTM-CRF	*
	4	BERT _{base}	‡
	5	BERT _{large}	‡
	6	RoBERTa	‡
	7	Electra _{base}	‡*
	8	Electra _{large}	‡*
	9	FLAT	Li et al. [44]‡‡
RE	10	BiGRU-Att	*
	11	BiLSTM-Att	*
	12	BiRNN-Att	*
	13	BERT _{base}	‡*
	14	BERT _{large}	‡*
	15	RoBERTa	‡*
	16	MTB	Baldini Soares et al. [6]†‡
JE	17	BERT _{wwm-ext}	Cui et al. [19]†‡
	18	CasRel _{BERT}	Wei et al. [73]†‡
	19	TPLinker _{BERT}	Wang et al. [70]†‡

Table 7: Part of employed datasets for well-tuning built-in models. ✓ indicates the dataset has annotation for the corresponding task.

id	Dataset	Language	Annotation		
			NER	RE	SPO
1	NYT[61]	English	✓	✓	✓
2	WebNLG[24]	English	✓	✓	✓
3	TACRED[86]	English	✓	✓	✓
4	CONLL[65]	English	✓		
5	DUIE2.0[43]	Chinese	✓	✓	✓
6	IPRE[69]	Chinese	✓	✓	✓
7	Resume[85]	Chinese	✓		

¹⁶In most cases, η is not sensitive to the result of cloud resource procurement and scheduling, and we recommend this default balanced scheduling strategy. Only when η converges to 1, the scheduler will adopt an aggressive resource procurement plan and scheduling scheme.

operator name	Description	Input	Output	configurable	programmable
entity type filter	Filter the entities according to configured entity type	entity, entity_type	&		✓
relation filter	Filter the relations according to configured relation list	relation, category	&		✓
score filter	Filter the entities or relations according to score located in meta info and configured threshold	entity/relation, category, metascore	&		✓
filter	Filter the entities, relations and entity pairs according to designed schema	*	&		✓
schema filter	Filter the entities, relations and entity pairs according to designed schema	*	&		✓
custom filter	Filter based on user programmed lambda function				
entity type mapper	Map the entity type according to the configured mapping	Class(entity_type)	&		✓
relation mapper	Map the relation according to the configured mapping	Relation(relation_category)	&		✓
mapper	custom mapper	Map the entity type or relation based on user programmed lambda function	*		✓
category ensemble (vote)	Model ensemble for multiple classification-based models based on majority vote	relation, category	&		
category ensemble (score)	Model ensemble for multiple classification-based models based on weighted score sum	relation, category, meta.score	&		✓
integrator	chunk ensemble	Integrate chunks like entities obtained from the multiple extraction-based models	entity, entity_type	&	
	data integrator	Integrate (merge) output data from different operators	*	&	
constructor	entity pair constructor	Construct the given entities into entity pairs via permutation	entity	entity_pair	
	triple constructor	Construct the given entity pairs and the corresponding relations into triple set	entity_pair, relation_category	triple	
controller	start	Denote the entrance of the flowline	/	sample	
	end	Denote the outlet of the flowline	*	/	
	NER	Extract the entities and the corresponding entity types from the samples	sample	entity, entity_type	
IE models	RE	Classify the relations of entity pairs according to given samples and entity pairs	sample, entity_pair	relation_category	
	JE	Extract entities and simultaneously determine the relationship between entities from given samples	sample	entity, entity_type	
	AE	Extract the attributes and attribute values of the specified entity from given samples	sample, entity	attribute, attribute_value	

Table 8: The commonly used built-in operators in gBuilder. (&) denotes the output is consistent with the input, (*) denotes the operator accepting any input type, (/) denotes there is no input or output.

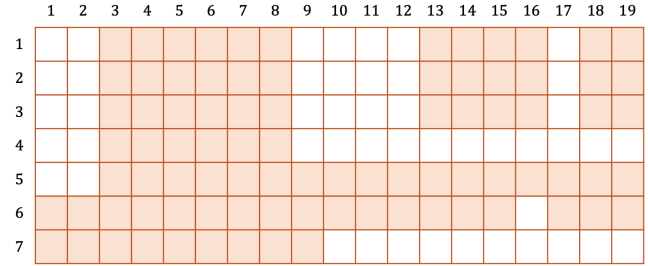


Figure 13: The "matrix" of built-in models, consists of the built-in models (columns) and the datasets (rows). The colored grid represents that the model has been trained and well-tuned on the corresponding dataset.

G BUILT-IN OPERATORS

gBuilder provides numerous necessary built-in operators for KGC. The most commonly used built-in operators and their descriptions are listed in Table 8.